

Measurements of Weak Decay Asymmetries of $\Lambda_c^+ \rightarrow pK_S^0$, $\Lambda\pi^+$, $\Sigma^+\pi^0$, and $\Sigma^0\pi^+$

M. Ablikim¹, M. N. Achasov^{10,d}, P. Adlarson⁵⁸, S. Ahmed¹⁵, M. Albrecht⁴, M. Alekseev^{57A,57C}, A. Amoroso^{57A,57C}, F. F. An¹, Q. An^{54,42}, Y. Bai⁴¹, O. Bakina²⁷, R. Baldini Ferroli^{23A}, Y. Ban³⁵, K. Begzsuren²⁵, J. V. Bennett⁵, N. Berger²⁶, M. Bertani^{23A}, D. Bettoni^{24A}, F. Bianchi^{57A,57C}, J. Biernat⁵⁸, J. Bloms⁵¹, I. Boyko²⁷, R. A. Briere⁵, H. Cai⁵⁹, X. Cai^{1,42}, A. Calcaterra^{23A}, G. F. Cao^{1,46}, N. Cao^{1,46}, S. A. Cetin^{45B}, J. Chai^{57C}, J. F. Chang^{1,42}, W. L. Chang^{1,46}, G. Chelkov^{27,b,c}, D. Y. Chen⁶, G. Chen¹, H. S. Chen^{1,46}, J. C. Chen¹, M. L. Chen^{1,42}, S. J. Chen³³, Y. B. Chen^{1,42}, W. Cheng^{57C}, G. Cibinetto^{24A}, F. Cossio^{57C}, X. F. Cui³⁴, H. L. Dai^{1,42}, J. P. Dai^{37,h}, X. C. Dai^{1,46}, A. Dbeyssi¹⁵, D. Dedovich²⁷, Z. Y. Deng¹, A. Denig²⁶, I. Denysenko²⁷, M. Destefanis^{57A,57C}, F. De Mori^{57A,57C}, Y. Ding³¹, C. Dong³⁴, J. Dong^{1,42}, L. Y. Dong^{1,46}, M. Y. Dong^{1,42,46}, Z. L. Dou³³, S. X. Du⁶², J. Z. Fan⁴⁴, J. Fang^{1,42}, S. S. Fang^{1,46}, Y. Fang¹, R. Farinelli^{24A,24B}, L. Fava^{57B,57C}, F. Feldbauer⁴, G. Felici^{23A}, C. Q. Feng^{54,42}, M. Fritsch⁴, C. D. Fu¹, Y. Fu¹, Q. Gao¹, X. L. Gao^{54,42}, Y. Gao⁵⁵, Y. Gao⁴⁴, Y. G. Gao⁶, Z. Gao^{54,42}, B. Garillon²⁶, I. Garzia^{24A}, E. M. Gersabeck⁴⁹, A. Gilman⁵⁰, K. Goetzen¹¹, L. Gong³⁴, W. X. Gong^{1,42}, W. Gradl²⁶, M. Greco^{57A,57C}, L. M. Gu³³, M. H. Gu^{1,42}, S. Gu Gu², Y. T. Gu¹³, A. Q. Guo²², L. B. Guo³², R. P. Guo^{1,46}, Y. P. Guo²⁶, A. Guskov²⁷, S. Han⁵⁹, X. Q. Hao¹⁶, F. A. Harris⁴⁷, K. L. He^{1,46}, F. H. Heinsius⁴, T. Held⁴, Y. K. Heng^{1,42,46}, Y. R. Hou⁴⁶, Z. L. Hou¹, H. M. Hu^{1,46}, J. F. Hu^{37,h}, T. Hu^{1,42,46}, Y. Hu¹, G. S. Huang^{54,42}, J. S. Huang¹⁶, X. T. Huang³⁶, X. Z. Huang³³, Z. L. Huang³¹, N. Huesken⁵¹, T. Hussain⁵⁶, W. Ikegami Andersson⁵⁸, W. Imoehl²², M. Irshad^{54,42}, Q. Ji¹, Q. P. Ji¹⁶, X. B. Ji^{1,46}, X. L. Ji^{1,42}, H. L. Jiang³⁶, X. S. Jiang^{1,42,46}, X. Y. Jiang³⁴, J. B. Jiao³⁶, Z. Jiao¹⁸, D. P. Jin^{1,42,46}, S. Jin³³, Y. Jin⁴⁸, T. Johansson⁵⁸, N. Kalantar-Nayestanaki²⁹, X. S. Kang³¹, R. Kappert²⁹, M. Kavatsyuk²⁹, B. C. Ke¹, I. K. Keshk⁴, T. Khan^{54,42}, A. Khoukaz⁵¹, P. Kiese²⁶, R. Kiuchi¹, R. Kliemt¹¹, L. Koch²⁸, O. B. Kolcu^{45B,f}, B. Kopf⁴, M. Kuemmel⁴, M. Kuessner⁴, A. Kupsc⁵⁸, M. Kurth¹, M. G. Kurth^{1,46}, W. Kühn²⁸, J. S. Lange²⁸, P. Larin¹⁵, L. Lavezzi^{57C}, H. Leithoff²⁶, T. Lenz²⁶, C. Li⁵⁸, Cheng Li^{54,42}, D. M. Li⁶², F. Li^{1,42}, F. Y. Li³⁵, G. Li¹, H. B. Li^{1,46}, H. J. Li^{9,j}, J. C. Li¹, J. W. Li⁴⁰, Ke Li¹, L. K. Li¹, Lei Li³, P. L. Li^{54,42}, P. R. Li³⁰, Q. Y. Li³⁶, W. D. Li^{1,46}, W. G. Li¹, X. H. Li^{54,42}, X. L. Li³⁶, X. N. Li^{1,42}, X. Q. Li³⁴, Z. B. Li⁴³, Z. Y. Li⁴³, H. Liang^{1,46}, H. Liang^{54,42}, Y. F. Liang³⁹, Y. T. Liang²⁸, G. R. Liao¹², L. Z. Liao^{1,46}, J. Libby²¹, C. X. Lin⁴³, D. X. Lin¹⁵, Y. J. Lin¹³, B. Liu^{37,h}, B. J. Liu¹, C. X. Liu¹, D. Liu^{54,42}, D. Y. Liu^{37,h}, F. H. Liu³⁸, Fang Liu¹, Feng Liu⁶, H. B. Liu¹³, H. M. Liu^{1,46}, Huanhuan Liu¹, Huihui Liu¹⁷, J. B. Liu^{54,42}, J. Y. Liu^{1,46}, K. Y. Liu³¹, Ke Liu⁶, Q. Liu⁴⁶, S. B. Liu^{54,42}, T. Liu^{1,46}, X. Liu³⁰, X. Y. Liu^{1,46}, Y. B. Liu³⁴, Z. A. Liu^{1,42,46}, Zhiqing Liu²⁶, Y. F. Long³⁵, X. C. Lou^{1,42,46}, H. J. Lu¹⁸, J. D. Lu^{1,46}, J. G. Lu^{1,42}, Y. Lu¹, Y. P. Lu^{1,42}, C. L. Luo³², M. X. Luo⁶¹, P. W. Luo⁴³, T. Luo^{9,j}, X. L. Luo^{1,42}, S. Lusso^{57C}, X. R. Lyu⁴⁶, F. C. Ma³¹, H. L. Ma¹, L. L. Ma³⁶, M. M. Ma^{1,46}, Q. M. Ma¹, X. N. Ma³⁴, X. X. Ma^{1,46}, X. Y. Ma^{1,42}, Y. M. Ma³⁶, F. E. Maas¹⁵, M. Maggiora^{57A,57C}, S. Maldaner²⁶, S. Malde⁵², Q. A. Malik⁵⁶, A. Mangoni^{23B}, Y. J. Mao³⁵, Z. P. Mao¹, S. Marcello^{57A,57C}, Z. X. Meng⁴⁸, J. G. Messchendorp²⁹, G. Mezzadri^{24A}, J. Min^{1,42}, T. J. Min³³, R. E. Mitchell²², X. H. Mo^{1,42,46}, Y. J. Mo⁶, C. Morales Morales¹⁵, N. Yu. Muchnoi^{10,d}, H. Muramatsu⁵⁰, A. Mustafa⁴, S. Nakhoul^{11,g}, Y. Nefedov²⁷, F. Nerling^{11,g}, I. B. Nikolaev^{10,d}, Z. Ning^{1,42}, S. Nisar^{8,k}, S. L. Niu^{1,42}, S. L. Olsen⁴⁶, Q. Ouyang^{1,42,46}, S. Pacetti^{23B}, Y. Pan^{54,42}, M. Papenbrock⁵⁸, P. Patteri^{23A}, M. Pelizaeus⁴, H. P. Peng^{54,42}, K. Peters^{11,g}, Y. Petterson⁵⁸, J. L. Ping³², R. G. Ping^{1,46}, A. Pitka⁴, R. Poling⁵⁰, V. Prasad^{54,42}, M. Qi³³, T. Y. Qi², S. Qian^{1,42}, C. F. Qiao⁴⁶, N. Qin⁵⁹, X. P. Qin¹³, X. S. Qin⁴, Z. H. Qin^{1,42}, J. F. Qiu¹, S. Q. Qu³⁴, K. H. Rashid^{56,i}, C. F. Redmer²⁶, M. Richter⁴, M. Ripka²⁶, A. Rivetti^{57C}, V. Rodin²⁹, M. Rolo^{57C}, G. Rong^{1,46}, Ch. Rosner¹⁵, M. Rump⁵¹, A. Sarantsev^{27,e}, M. Savrie^{24B}, K. Schoenning⁵⁸, W. Shan¹⁹, X. Y. Shan^{54,42}, M. Shao^{54,42}, C. P. Shen², P. X. Shen³⁴, X. Y. Shen^{1,46}, H. Y. Sheng¹, X. Shi^{1,42}, X. D. Shi^{54,42}, J. J. Song³⁶, Q. Q. Song^{54,42}, X. Y. Song¹, S. Sosio^{57A,57C}, C. Sowa⁴, S. Spataro^{57A,57C}, F. F. Sui³⁶, G. X. Sun¹, J. F. Sun¹⁶, L. Sun⁵⁹, S. S. Sun^{1,46}, X. H. Sun¹, Y. J. Sun^{54,42}, Y. K. Sun^{54,42}, Y. Z. Sun¹, Z. J. Sun^{1,42}, Z. T. Sun¹, Y. T. Tan^{54,42}, C. J. Tang³⁹, G. Y. Tang¹, X. Tang¹, V. Thoren⁵⁸, B. Tsednee²⁵, I. Uman^{45D}, B. Wang¹, B. L. Wang⁴⁶, C. W. Wang³³, D. Y. Wang³⁵, H. H. Wang³⁶, K. Wang^{1,42}, L. L. Wang¹, L. S. Wang¹, M. Wang³⁶, M. Z. Wang³⁵, Meng Wang^{1,46}, P. L. Wang¹, R. M. Wang⁶⁰, W. P. Wang^{54,42}, X. Wang³⁵, X. F. Wang¹, X. L. Wang^{9,j}, Y. Wang^{54,42}, Y. Wang⁴³, Y. F. Wang^{1,42,46}, Z. Wang^{1,42}, Z. G. Wang^{1,42}, Z. Y. Wang¹, Zongyuan Wang^{1,46}, T. Weber⁴, D. H. Wei¹², P. Weidenkaff²⁶, H. W. Wen³², S. P. Wen¹, U. Wiedner⁴, G. Wilkinson⁵², M. Wolke⁵⁸, L. H. Wu¹, L. J. Wu^{1,46}, Z. Wu^{1,42}, L. Xia^{54,42}, Y. Xia²⁰, S. Y. Xiao¹, Y. J. Xiao^{1,46}, Z. J. Xiao³², Y. G. Xie^{1,42}, Y. H. Xie⁶, T. Y. Xing^{1,46}, X. A. Xiong^{1,46}, Q. L. Xiu^{1,42}, G. F. Xu¹, L. Xu¹, Q. J. Xu¹⁴, W. Xu^{1,46}, X. P. Xu⁴⁰, F. Yan⁵⁵, L. Yan^{57A,57C}, W. B. Yan^{54,42}, W. C. Yan², Y. H. Yan²⁰, H. J. Yang^{37,h}, H. X. Yang¹, L. Yang⁵⁹, R. X. Yang^{54,42}, S. L. Yang^{1,46}, Y. H. Yang³³, Y. X. Yang¹², Yifan Yang^{1,46}, Z. Q. Yang²⁰, M. Ye^{1,42}, M. H. Ye⁷, J. H. Yin¹, Z. Y. You⁴³, B. X. Yu^{1,42,46}, C. X. Yu³⁴, J. S. Yu²⁰, C. Z. Yuan^{1,46}, X. Q. Yuan³⁵, Y. Yuan¹, A. Yuncu^{45B,a}, A. A. Zafar⁵⁶, Y. Zeng²⁰, B. X. Zhang¹, B. Y. Zhang^{1,42}, C. C. Zhang¹, D. H. Zhang¹, H. H. Zhang⁴³, H. Y. Zhang^{1,42}, J. Zhang^{1,46}, J. L. Zhang⁶⁰, J. Q. Zhang⁴, J. W. Zhang^{1,42,46}, J. Y. Zhang¹, J. Z. Zhang^{1,46}, K. Zhang^{1,46}, L. Zhang⁴⁴, S. F. Zhang³³, T. J. Zhang^{37,h}, X. Y. Zhang³⁶, Y. Zhang^{54,42}, Y. H. Zhang^{1,42}, Y. T. Zhang^{54,42}, Yang Zhang¹, Yao Zhang¹, Yi Zhang^{9,j}, Yu Zhang⁴⁶, Z. H. Zhang⁶, Z. P. Zhang⁵⁴, Z. Y. Zhang⁵⁹, G. Zhao¹, J. W. Zhao^{1,42}, J. Y. Zhao^{1,46}, J. Z. Zhao^{1,42}, Lei Zhao^{54,42}, Ling Zhao¹, M. G. Zhao³⁴, Q. Zhao¹, S. J. Zhao⁶², T. C. Zhao¹, Y. B. Zhao^{1,42}, Z. G. Zhao^{54,42}, A. Zhemchugov^{27,b}, B. Zheng⁵⁵, J. P. Zheng^{1,42}, Y. Zheng³⁵, Y. H. Zheng⁴⁶, B. Zhong³², L. Zhou^{1,42}, L. P. Zhou^{1,46}, Q. Zhou^{1,46}, X. Zhou⁵⁹, X. K. Zhou⁴⁶, X. R. Zhou^{54,42}, Xiaoyu Zhou²⁰, Xu Zhou²⁰, A. N. Zhu^{1,46}, J. Zhu³⁴, J. Zhu⁴³, K. Zhu¹, K. J. Zhu^{1,42,46}, S. H. Zhu⁵³, W. J. Zhu³⁴, X. L. Zhu⁴⁴, Y. C. Zhu^{54,42}, Y. S. Zhu^{1,46}, Z. A. Zhu^{1,46}, J. Zhuang^{1,42}, B. S. Zou¹, J. H. Zou¹

(BESIII Collaboration)

¹ Institute of High Energy Physics, Beijing 100049, People's Republic of China² Beihang University, Beijing 100191, People's Republic of China³ Beijing Institute of Petrochemical Technology, Beijing 102617, People's Republic of China

- ⁴ Bochum Ruhr-University, D-44780 Bochum, Germany
- ⁵ Carnegie Mellon University, Pittsburgh, Pennsylvania 15213, USA
- ⁶ Central China Normal University, Wuhan 430079, People's Republic of China
- ⁷ China Center of Advanced Science and Technology, Beijing 100190, People's Republic of China
- ⁸ COMSATS University Islamabad, Lahore Campus, Defence Road, Off Raiwind Road, 54000 Lahore, Pakistan
- ⁹ Fudan University, Shanghai 200443, People's Republic of China
- ¹⁰ G.I. Budker Institute of Nuclear Physics SB RAS (BINP), Novosibirsk 630090, Russia
- ¹¹ GSI Helmholtzcentre for Heavy Ion Research GmbH, D-64291 Darmstadt, Germany
- ¹² Guangxi Normal University, Guilin 541004, People's Republic of China
- ¹³ Guangxi University, Nanning 530004, People's Republic of China
- ¹⁴ Hangzhou Normal University, Hangzhou 310036, People's Republic of China
- ¹⁵ Helmholtz Institute Mainz, Johann-Joachim-Becher-Weg 45, D-55099 Mainz, Germany
- ¹⁶ Henan Normal University, Xinxiang 453007, People's Republic of China
- ¹⁷ Henan University of Science and Technology, Luoyang 471003, People's Republic of China
- ¹⁸ Huangshan College, Huangshan 245000, People's Republic of China
- ¹⁹ Hunan Normal University, Changsha 410081, People's Republic of China
- ²⁰ Hunan University, Changsha 410082, People's Republic of China
- ²¹ Indian Institute of Technology Madras, Chennai 600036, India
- ²² Indiana University, Bloomington, Indiana 47405, USA
- ²³ (A)INFN Laboratori Nazionali di Frascati, I-00044, Frascati, Italy; (B)INFN and University of Perugia, I-06100, Perugia, Italy
- ²⁴ (A)INFN Sezione di Ferrara, I-44122, Ferrara, Italy; (B)University of Ferrara, I-44122, Ferrara, Italy
- ²⁵ Institute of Physics and Technology, Peace Ave. 54B, Ulaanbaatar 13330, Mongolia
- ²⁶ Johannes Gutenberg University of Mainz, Johann-Joachim-Becher-Weg 45, D-55099 Mainz, Germany
- ²⁷ Joint Institute for Nuclear Research, 141980 Dubna, Moscow region, Russia
- ²⁸ Justus-Liebig-Universitaet Giessen, II. Physikalisches Institut, Heinrich-Buff-Ring 16, D-35392 Giessen, Germany
- ²⁹ KVI-CART, University of Groningen, NL-9747 AA Groningen, The Netherlands
- ³⁰ Lanzhou University, Lanzhou 730000, People's Republic of China
- ³¹ Liaoning University, Shenyang 110036, People's Republic of China
- ³² Nanjing Normal University, Nanjing 210023, People's Republic of China
- ³³ Nanjing University, Nanjing 210093, People's Republic of China
- ³⁴ Nankai University, Tianjin 300071, People's Republic of China
- ³⁵ Peking University, Beijing 100871, People's Republic of China
- ³⁶ Shandong University, Jinan 250100, People's Republic of China
- ³⁷ Shanghai Jiao Tong University, Shanghai 200240, People's Republic of China
- ³⁸ Shanxi University, Taiyuan 030006, People's Republic of China
- ³⁹ Sichuan University, Chengdu 610064, People's Republic of China
- ⁴⁰ Soochow University, Suzhou 215006, People's Republic of China
- ⁴¹ Southeast University, Nanjing 211100, People's Republic of China
- ⁴² State Key Laboratory of Particle Detection and Electronics, Beijing 100049, Hefei 230026, People's Republic of China
- ⁴³ Sun Yat-Sen University, Guangzhou 510275, People's Republic of China
- ⁴⁴ Tsinghua University, Beijing 100084, People's Republic of China
- ⁴⁵ (A)Ankara University, 06100 Tandogan, Ankara, Turkey; (B)Istanbul Bilgi University, 34060 Eyup, Istanbul, Turkey; (C)Uludag University, 16059 Bursa, Turkey; (D)Near East University, Nicosia, North Cyprus, Mersin 10, Turkey
- ⁴⁶ University of Chinese Academy of Sciences, Beijing 100049, People's Republic of China
- ⁴⁷ University of Hawaii, Honolulu, Hawaii 96822, USA
- ⁴⁸ University of Jinan, Jinan 250022, People's Republic of China
- ⁴⁹ University of Manchester, Oxford Road, Manchester, M13 9PL, United Kingdom
- ⁵⁰ University of Minnesota, Minneapolis, Minnesota 55455, USA
- ⁵¹ University of Muenster, Wilhelm-Klemm-Str. 9, 48149 Muenster, Germany
- ⁵² University of Oxford, Keble Rd, Oxford, UK OX13RH
- ⁵³ University of Science and Technology Liaoning, Anshan 114051, People's Republic of China
- ⁵⁴ University of Science and Technology of China, Hefei 230026, People's Republic of China
- ⁵⁵ University of South China, Hengyang 421001, People's Republic of China
- ⁵⁶ University of the Punjab, Lahore-54590, Pakistan
- ⁵⁷ (A)University of Turin, I-10125, Turin, Italy; (B)University of Eastern Piedmont, I-15121, Alessandria, Italy; (C)INFN, I-10125, Turin, Italy
- ⁵⁸ Uppsala University, Box 516, SE-75120 Uppsala, Sweden
- ⁵⁹ Wuhan University, Wuhan 430072, People's Republic of China
- ⁶⁰ Xinyang Normal University, Xinyang 464000, People's Republic of China
- ⁶¹ Zhejiang University, Hangzhou 310027, People's Republic of China
- ⁶² Zhengzhou University, Zhengzhou 450001, People's Republic of China

^a Also at Bogazici University, 34342 Istanbul, Turkey

^b Also at the Moscow Institute of Physics and Technology, Moscow 141700, Russia

^c Also at the Functional Electronics Laboratory, Tomsk State University, Tomsk, 634050, Russia

^d Also at the Novosibirsk State University, Novosibirsk, 630090, Russia

^e Also at the NRC "Kurchatov Institute", PNPI, 188300, Gatchina, Russia

^f Also at Istanbul Arel University, 34295 Istanbul, Turkey

^g Also at Goethe University Frankfurt, 60323 Frankfurt am Main, Germany

^h Also at Key Laboratory for Particle Physics, Astrophysics and Cosmology, Ministry of Education; Shanghai Key Laboratory for Particle Physics and Cosmology; Institute of Nuclear and Particle Physics, Shanghai 200240, People's Republic of China

ⁱ Also at Government College Women University, Sialkot - 51310. Punjab, Pakistan.

^j Also at Key Laboratory of Nuclear Physics and Ion-beam Application (MOE) and Institute of Modern Physics, Fudan University, Shanghai 200443, People's Republic of China

^k Also at Harvard University, Department of Physics, Cambridge, MA, 02138, USA

(Dated: May 14, 2019)

Using $e^+e^- \rightarrow \Lambda_c^+ \bar{\Lambda}_c^-$ production from a 567 pb^{-1} data sample collected by BESIII at 4.6 GeV, a full angular analysis is carried out simultaneously on the four decay modes of $\Lambda_c^+ \rightarrow pK_S^0$, $\Lambda\pi^+$, $\Sigma^+\pi^0$, and $\Sigma^0\pi^+$. For the first time, the Λ_c^+ transverse polarization is studied in unpolarized e^+e^- collisions, where a non-zero effect is observed with a statistical significance of 2.1σ . The decay asymmetry parameters of the Λ_c^+ weak hadronic decays into pK_S^0 , $\Lambda\pi^+$, $\Sigma^+\pi^0$ and $\Sigma^0\pi^+$ are measured to be $0.18 \pm 0.43(\text{stat}) \pm 0.14(\text{syst})$, $-0.80 \pm 0.11(\text{stat}) \pm 0.02(\text{syst})$, $-0.57 \pm 0.10(\text{stat}) \pm 0.07(\text{syst})$, and $-0.73 \pm 0.17(\text{stat}) \pm 0.07(\text{syst})$, respectively. In comparison with previous results, the measurements for the $\Lambda\pi^+$ and $\Sigma^+\pi^0$ modes are consistent but with improved precision, while the parameters for the pK_S^0 and $\Sigma^0\pi^+$ modes are measured for the first time.

The study of the lightest charmed baryon Λ_c^+ is important for the understanding of the whole charmed baryon sector. In recent years, there has been significant progress in studying the Λ_c^+ , both experimentally and theoretically [1, 2]. This provides crucial information in detailed explorations of the singly charmed baryons (Σ_c , Ξ_c and Ω_c) [3, 4], and further searches or discoveries of the doubly charmed baryons (Ξ_{cc} and Ω_{cc}) [5, 6]. Moreover, as the charmed baryon is the favored weak decay final state of b -baryons and its properties are inputs to study b -baryons, improved knowledge in the charm sector can contribute substantially to understanding the properties of b -baryons.

Some QCD-inspired charmed baryon models that have been developed [7] are the flavor symmetry model [8], factorization model [9], pole model [10], and current algebra framework [11]. As shown in Refs. [2, 7], many of these models calculate Λ_c^+ decay rates in good agreement with experimental results. But the decay asymmetries predicted by these models for Λ_c^+ two-body hadronic weak decays do not agree very well.

The decay asymmetry parameter, α_{BP}^+ , in a weak decay $\Lambda_c^+ \rightarrow BP$ (B denotes a $J^P = \frac{1}{2}^+$ baryon and P denotes a $J^P = 0^-$ pseudoscalar meson) is defined as $\alpha_{BP}^+ \equiv \frac{2\text{Re}(s \cdot p)}{|s|^2 + |p|^2}$, where s and p stand for the parity-violating s -wave and parity-conserving p -wave amplitudes in the decay, respectively. Model calculations of α_{BP}^+ in $\Lambda_c^+ \rightarrow pK_S^0$, $\Lambda\pi^+$, $\Sigma^+\pi^0$, and $\Sigma^0\pi^+$ are listed in Table I, which shows large variations among the different models. As predictions of α_{BP}^+ rely on the relative phase between the two amplitudes, the experimental measurements of the decay asymmetry parameters serve as very sensitive probes to test different theoretical models.

Experimentally, only $\alpha_{\Lambda\pi^+}^+$ and $\alpha_{\Sigma^+\pi^0}^+$ have been measured previously [12–15]. The measured value for $\alpha_{\Sigma^+\pi^0}^+$

is -0.45 ± 0.32 , in contradiction with the predicted values in many theoretical models [10, 11, 16–19]. Therefore, it is important to carry out independent measurements of $\alpha_{\Sigma^+\pi^0}^+$ to confirm the sign of $\alpha_{\Sigma^+\pi^0}^+$ and test these models. Moreover, $\alpha_{\Sigma^+\pi^0}^+$ and $\alpha_{\Sigma^0\pi^+}^+$ should have the same value according to hyperon isospin symmetry [20], and any deviation from this expectation provides critical information on final state interactions in Λ_c^+ hadronic decays. All the models predict $\alpha_{\Lambda\pi^+}^+$ consistent with the measured values, and it is necessary to further improve the experimental precision to discriminate between them.

In previous experiments, Λ_c^+ was assumed to be unpolarized, and the decay asymmetry parameter α_{BP}^+ was obtained by analyzing the longitudinal polarization from the weak two-body decay of the produced baryon B , such as $\Lambda \rightarrow p\pi^-$ and $\Sigma^+ \rightarrow p\pi^0$ for $\alpha_{\Lambda\pi^+}^+$ and $\alpha_{\Sigma^+\pi^0}^+$, respectively. However, the hypothesis of unpolarized Λ_c^+ may not be valid. There have been observations of transverse Λ polarization in inclusive Λ production in e^+e^- collisions at 10.58 GeV [21] and in $e^+e^- \rightarrow \Lambda\bar{\Lambda}$ at J/ψ mass position [22], and it has been postulated that the produced Λ_c^+ could be polarized [23]. Further, as the polarization of the proton in the decay $\Lambda_c^+ \rightarrow pK_S^0$ is not accessible with the above method, a non-zero transverse polarization of the Λ_c^+ provides an alternative way to measure $\alpha_{pK_S^0}^+$ [24].

In this Letter, we investigate for the first time the transverse polarization of the Λ_c^+ baryon in unpolarized e^+e^- annihilations. We present for the first time measurements of the decay asymmetry parameters in Λ_c^+ decays into pK_S^0 , $\Lambda\pi^+$, $\Sigma^+\pi^0$, and $\Sigma^0\pi^+$ based on a multi-dimensional angular analysis of the cascade-decay final states, which greatly improves the resulting precision. Data sample used in this analysis corresponds to an integrated luminosity of 567 pb^{-1} collected with the BESIII

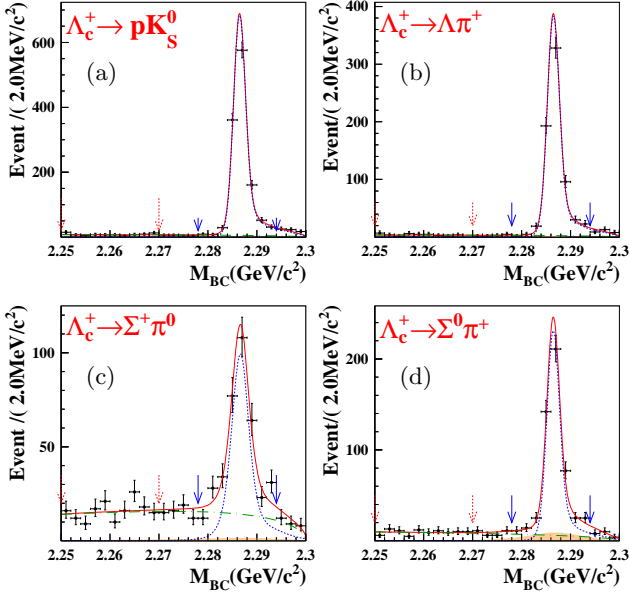


FIG. 1. (color online) Fits to the M_{BC} spectra of the signal candidates of (a) $\Lambda_c^+ \rightarrow pK_S^0$, (b) $\Lambda_c^+ \rightarrow \Lambda\pi^+$, (c) $\Lambda_c^+ \rightarrow \Sigma^+\pi^0$, and (d) $\Lambda_c^+ \rightarrow \Sigma^0\pi^+$. Points with error bars correspond to data, solid lines are the fitting curves, dashed lines describe the signal events distribution, dash-dotted lines show the Type-II backgrounds and shadowed areas correspond to Type-I backgrounds. Dashed and solid arrows show the sideband and signal regions, respectively.

detector at BEPCII at center-of-mass (CM) energy of 4.6 GeV.

Since the close proximity of the CM energy to the $\Lambda_c^+\bar{\Lambda}_c^-$ mass threshold does not allow an additional hadron to be produced, $\Lambda_c^+\bar{\Lambda}_c^-$ are always generated in pairs, which provides a clean environment to study their decays. When one Λ_c^+ is detected, another $\bar{\Lambda}_c^-$ partner is inferred. Hence, to increase signal yields, we adopt a partial reconstruction method, in which only one Λ_c^+ is reconstructed out of all the final-state particles in an event. The charge conjugation modes are always implied in the context, unless otherwise stated explicitly.

Details of the BESIII apparatus, the software framework and the Monte Carlo (MC) simulation sample have been given in Ref. [25]. The Λ_c^+ signal candidates are reconstructed through the decays into pK_S^0 , $\Lambda\pi^+$, $\Sigma^+\pi^0$ and $\Sigma^0\pi^+$. Here, the intermediate particles K_S^0 , Λ , Σ^+ , Σ^0 and π^0 are reconstructed via the decays $K_S^0 \rightarrow \pi^+\pi^-$, $\Lambda \rightarrow p\pi^-$, $\Sigma^+ \rightarrow p\pi^0$, $\Sigma^0 \rightarrow \gamma\Lambda$, and $\pi^0 \rightarrow \gamma\gamma$. The event selection criteria follow those described in Ref. [25], unless otherwise stated explicitly. To suppress the $\Lambda_c^+ \rightarrow pK_S^0$, $K_S^0 \rightarrow \pi^0\pi^0$ events in the $\Sigma^+\pi^0$ candidate samples, the invariant mass of the $\pi^0\pi^0$ system is required to be outside the range [400, 550] MeV/ c^2 .

For each signal decay mode, the yields are obtained from a fit to the beam-constrained mass (M_{BC}) distribution, $M_{BC} \equiv \sqrt{E_{\text{beam}}^2 - p_{\Lambda_c^+}^2}$, where E_{beam} is the aver-

age beam energy and $p_{\Lambda_c^+}$ is the measured Λ_c^+ momentum in the CM system of the e^+e^- collisions. If more than one candidate is reconstructed in the event, the one with the smallest energy difference ($|\Delta E|$) is kept, where $\Delta E \equiv E_{\Lambda_c^+} - E_{\text{beam}}$, and $E_{\Lambda_c^+}$ is the measured total energy of the Λ_c^+ candidate.

Figure 1 shows the M_{BC} distributions for the signal candidates, where the Λ_c^+ signal peak is evident at the nominal Λ_c^+ mass. The backgrounds can be classified into two types. The Type-I backgrounds are from the true Λ_c^+ signal decays, where at least one of the final state particle candidates is wrongly assigned in reconstruction. The Type-II backgrounds correspond to combinatorial backgrounds mostly from $e^+e^- \rightarrow q\bar{q}$ ($q = u, d, s$) processes. To evaluate the Type-I and Type-II background level, unbinned maximum likelihood fits (shown in Fig. 1) are applied to the M_{BC} spectra. The signal and Type-I background shapes, as well as the ratio of their yields, are derived from the signal MC simulation samples. These two shapes are convolved with a common Gaussian function, whose width is left free and represents the difference in resolution between data and MC simulations. The Type-II background shape is modeled by an ARGUS function [26]. The Λ_c^+ signal and sideband regions are chosen as [2.278, 2.294] GeV/ c^2 and [2.250, 2.270] GeV/ c^2 , respectively.

The decay asymmetry parameters are determined by analyzing the multi-dimensional angular distributions, where the full cascade decay chains are considered. The full angular dependence formulae (4), (6), and (10) in Ref. [24], constructed under the helicity basis, are used in the fit. To illustrate the helicity system defined in this analysis, we take as an example the two-level cascade decay process $\Lambda_c^+ \rightarrow \Lambda\pi^+$, $\Lambda \rightarrow p\pi^-$ following the level-0 process $e^+e^- \rightarrow \gamma^* \rightarrow \Lambda_c^+\bar{\Lambda}_c^-$. An analogous formalism is applied to the other $\Lambda_c^+ \rightarrow BP$ decays.

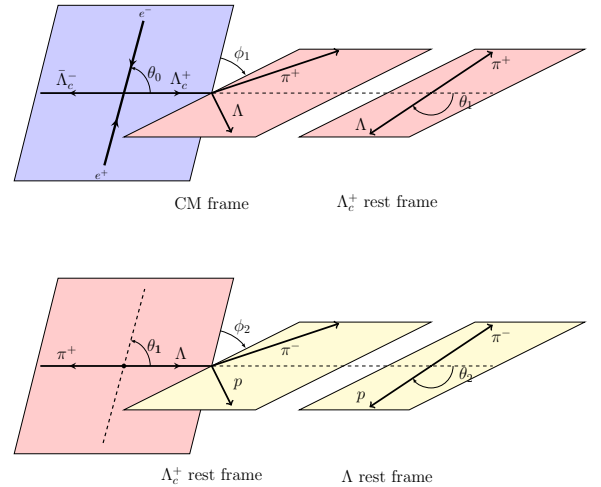


FIG. 2. (color online) Definition of the helicity frame for $e^+e^- \rightarrow \Lambda_c^+\bar{\Lambda}_c^-$, $\Lambda_c^+ \rightarrow \Lambda\pi^+$, $\Lambda \rightarrow p\pi^-$

Figure 2 illustrates the definitions of the full system of helicity angles for the $\Lambda_c^+ \rightarrow \Lambda\pi^+$ mode. In the helicity frame of $e^+e^- \rightarrow \Lambda_c^+\bar{\Lambda}_c^-$, θ_0 is the polar angle of the Λ_c^+ with respect to the e^+ beam axis in the e^+e^- CM system. For the helicity angles of the $\Lambda_c^+ \rightarrow \Lambda\pi^+$ decay, ϕ_1 is the angle between the $e^+\Lambda_c^+$ and $\Lambda\pi^+$ planes, and θ_1 is the polar angle of the Λ momentum in the rest frame of the Λ_c^+ with respect to the Λ_c^+ momentum in the CM frame. The angle subscript represents the level numbering of the cascade signal decays. For the helicity angles describing the $\Lambda \rightarrow p\pi^+$ decay, ϕ_2 is the angle between the $\Lambda\pi^+$ plane and $p\pi^-$ plane and θ_2 is the polar angle of the proton momentum with respect to opposite direction of π^+ momentum in the rest frame of Λ . For the three-level cascade decays $\Lambda_c^+ \rightarrow \Sigma^0\pi^+$, $\Sigma^0 \rightarrow \Lambda\gamma$, $\Lambda \rightarrow p\pi^-$ process, ϕ_3 is the angle between the $\Lambda\gamma$ and $p\pi^-$ planes, while θ_3 is the polar angle of the proton with respect to the opposite direction of the photon momentum (from $\Sigma^0 \rightarrow \Lambda\gamma$) in the rest frame of Λ .

In Ref. [24], we define Δ_0 as the phase angle difference between two individual helicity amplitudes, H_{λ_1, λ_2} , for the Λ_c^+ production process $\gamma^* \rightarrow \Lambda_c^+(\lambda_1)\bar{\Lambda}_c^-(\lambda_2)$ with total helicities $|\lambda_1 - \lambda_2| = 0$ and 1, respectively. In the case where one-photon exchange dominates the production process, Δ_0 is also the phase between the electric and magnetic form factors of the Λ_c^+ [23, 27]. The transverse polarization observable of the produced Λ_c^+ can be defined as

$$\mathcal{P}_T(\cos\theta_0) \equiv \sqrt{1 - \alpha_0^2} \cos\theta_0 \sin\theta_0 \sin\Delta_0, \quad (1)$$

whose magnitude varies as a function of $\cos\theta_0$. Similarly, two parameters, α_{BP}^+ and Δ_1^{BP} , describe the level-1 decays $\Lambda_c^+ \rightarrow \Lambda\pi^+$, $\Sigma^+\pi^0$, and $\Sigma^0\pi^+$, where Δ_1^{BP} is the phase angle difference between the two helicity amplitudes in the BP mode. The Lee-Yang parameters [24, 28] can be obtained with the relations

$$\begin{aligned} \beta_{BP} &= \sqrt{1 - (\alpha_{BP}^+)^2} \sin\Delta_1^{BP}, \\ \gamma_{BP} &= \sqrt{1 - (\alpha_{BP}^+)^2} \cos\Delta_1^{BP}. \end{aligned} \quad (2)$$

In the angular analysis, the free parameters describing the angular distributions for the four data sets are determined from a simultaneous unbinned maximum likelihood fit, as α_0 and Δ_0 are common. The likelihood function is constructed from the probability density function (PDF) jointly by

$$\mathcal{L}_{\text{data}} = \prod_{i=1}^{N_{\text{data}}} f_S(\vec{\xi}). \quad (3)$$

Here, $f_S(\vec{\xi})$ is the PDF of the signal process, N_{data} is the number of the events in data and i is event index. Signal PDF $f_S(\vec{\xi})$ is formulated as

$$f_S(\vec{\xi}) = \frac{\epsilon(\vec{\xi})|M(\vec{\xi}; \vec{\eta})|^2}{\int \epsilon(\vec{\xi})|M(\vec{\xi}; \vec{\eta})|^2 d\vec{\xi}}, \quad (4)$$

where the variable $\vec{\xi}$ denotes the kinematic angular observables, and $\vec{\eta}$ denotes the free parameters to be determined. $M(\vec{\xi})$ is the total decay amplitude [24] and $\epsilon(\vec{\xi})$ is the detection efficiency parameterized in terms of the kinematic variables $\vec{\xi}$. The background contribution to the joint likelihood is subtracted according to the calculated likelihoods for the Type-I background based on inclusive MC simulations and for the Type-II background according to the M_{BC} sideband. The MC-integration technique is adopted to compute the normalization factor as follows

$$\int \epsilon(\vec{\xi})|M(\vec{\xi}; \vec{\eta})|^2 d\vec{\xi} = \frac{1}{N_{\text{gen}}} \sum_{k_{\text{MC}}}^{N_{\text{MC}}} |M(\vec{\xi}_k; \vec{\eta})|^2, \quad (5)$$

where N_{gen} is the total number of MC-simulated signal events. N_{MC} is the number of the MC signal events survived from the full selection criteria and k_{MC} is its event index.

Minimization of the negative logarithmic likelihood with background subtraction over all the four signal processes is carried out using the MINUIT package [29]. Here, α_0 is fixed to the known value -0.20 [27]. For the charge-conjugation $\bar{\Lambda}_c^-$ decays, under the assumption of CP conservation, $\bar{\Delta}_0 = \Delta_0$, $\alpha_{BP}^+ = -\alpha_{BP}^-$, and $\bar{\Delta}_1^{BP} = -\Delta_1^{BP}$. The decay asymmetry parameter α_Λ for $\Lambda \rightarrow p\pi^-$ is taken from the recent BESIII measurement [22] and α_{Σ^+} for $\Sigma^+ \rightarrow p\pi^0$ from the Particle Data Group (PDG) [2]. From the fit, we obtain $\sin\Delta_0 = -0.28 \pm 0.13(\text{stat.})$ which differs from zero with a statistical significance of 2.1σ according to a likelihood ratio test. This indicates that transverse polarization \mathcal{P}_T of the Λ_c^+ is non-zero when $\sin(2\theta_0) \neq 0$. The numerical fit results are given in Table I, together with the calculated γ_{BP} and β_{BP} .

In Fig. 3, the fit results are illustrated using several projection variables. The real data are compared with the MC generated events re-weighted according to the fit.

For the $\Lambda_c^+ \rightarrow \Lambda\pi^+$ and $\Sigma^+\pi^0$ decays, if all angles are integrated over except for the angle θ_2 , the decay rate becomes [32]

$$\frac{dN}{d\cos\theta_2} \propto 1 + \alpha_{\Lambda\pi^+}^+ (\alpha_{\Sigma^+\pi^0}^+ \alpha_{\Sigma^+}) \cos\theta_2. \quad (6)$$

Equation (6) shows a characteristically longitudinal polarization of the produced $\Lambda(\Sigma^+)$ from the Λ_c^+ decays, and the asymmetry of $\cos\theta_2$ distribution reflects the product of the decay asymmetries $\alpha_{\Lambda\pi^+}^+ \alpha_\Lambda (\alpha_{\Sigma^+\pi^0}^+ \alpha_{\Sigma^+})$ [33]. The distributions of $\cos\theta_2$ in the $\Lambda_c^+ \rightarrow \Lambda\pi^+$ and $\Sigma^+\pi^0$ modes are shown in Figs. 3(a) and (b), respectively. The drop at the right side in Fig. 3(b) is due to the $K_S^0 \rightarrow \pi^0\pi^0$ veto.

For the $\Lambda_c^+ \rightarrow \Sigma^0\pi^+$ decay, the correlations of $\cos\theta_2$ and $\cos\theta_3$ in the subsequent level-2 decay $\Sigma^0 \rightarrow \gamma\Lambda$ and level-3 decay $\Lambda \rightarrow p\pi^-$, are shown in Figs. 3(c) and (d), respectively. The correlation of the average value of $\cos\theta_i$

TABLE I. Comparisons between different theoretical calculations and experimental measurements.

$\Lambda_c^+ \rightarrow$		pK_S^0	$\Lambda\pi^+$	$\Sigma^+\pi^0$	$\Sigma^0\pi^+$
α_{BP}^+	Predicted	-1.0 [16], 0.51 [11]	-0.70 [16], -0.67 [11]	0.71 [16], 0.92 [11]	0.70 [16], 0.92 [11]
		-0.49 [10], -0.90 [10]	-0.95 [10], -0.99 [10]	0.79 [10], -0.49 [10]	0.78 [10], -0.49 [10]
		-0.49 [17], -0.97 [18]	-0.96 [17], -0.95 [18]	0.83 [17], 0.43 [18]	0.83 [17], 0.43 [18]
		-0.66 [19], -0.90 [30]	-0.99 [19], -0.86 [30]	0.39 [19], -0.76 [30]	0.39 [19], -0.76 [30]
	-0.99 [20], -0.91 [31]	-0.99 [20], -0.94 [31]	-0.31 [20], -0.47 [31]	-0.31 [20], -0.47 [31]	
PDG [2]		-0.91 \pm 0.15	-0.45 \pm 0.32		
This work		0.18 \pm 0.43 \pm 0.14	-0.80 \pm 0.11 \pm 0.02	-0.57 \pm 0.10 \pm 0.07	-0.73 \pm 0.17 \pm 0.07
Δ_1^{BP} (rad)	This work		3.0 \pm 2.4 \pm 1.0	4.1 \pm 1.1 \pm 0.6	0.8 \pm 1.2 \pm 0.2
β_{BP}	This work		0.06 $^{+0.58+0.05}_{-0.47-0.06}$	-0.66 $^{+0.46+0.22}_{-0.25-0.02}$	0.48 $^{+0.35+0.07}_{-0.57-0.13}$
γ_{BP}	This work		-0.60 $^{+0.96+0.17}_{-0.05-0.03}$	-0.48 $^{+0.45+0.21}_{-0.42-0.04}$	0.49 $^{+0.35+0.07}_{-0.56-0.12}$

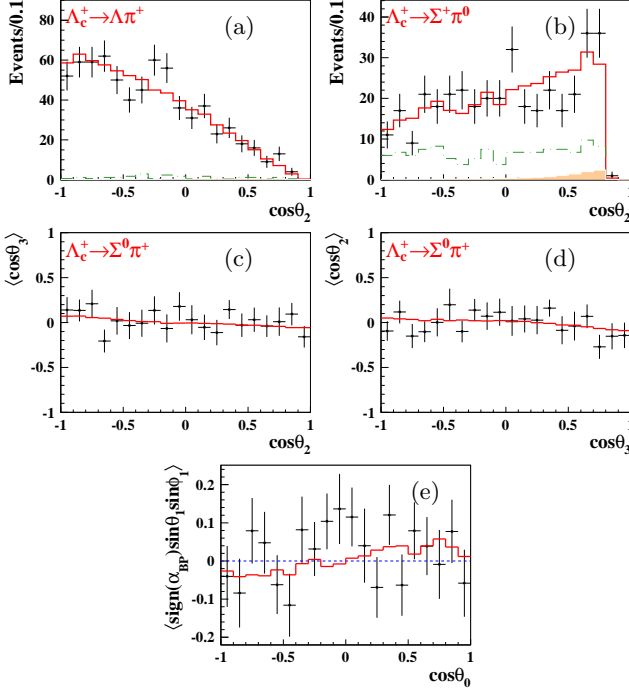


FIG. 3. (color online) $\cos\theta_2$ distributions in (a) $\Lambda\pi^+$, and (b) $\Sigma^+\pi^0$; (c) average value of $\cos\theta_3$ as a function of $\cos\theta_2$, and (d) average value of $\cos\theta_3$ as a function of $\cos\theta_3$ in $\Lambda_c^+ \rightarrow \Sigma^0\pi^+$; (e) $\langle \text{sign}(\alpha_{BP}) \sin\theta_1 \sin\phi_1 \rangle$ as a function of $\cos\theta_0$ for all the four signal channels. Points with error bars correspond to data; (red) solid lines represent the MC-determined shapes taking into account the fit results; (green) dash-dotted lines represent the Type-II background and shaded histograms show the Type-I background.

satisfies the relation

$$\langle \cos\theta_i \rangle = -\frac{1}{6} \alpha_{\Sigma^0\pi^+}^+ \alpha_{\Lambda} \cos\theta_j, \quad (7)$$

with $(i, j) = (2, 3)$ or $(3, 2)$.

If the full expressions for the joint angular distributions (Ref. [24]) are integrated over the angles of the level 2 and 3 decay products, the remaining partial decay rate \mathcal{W} is

$$\mathcal{W} \propto 1 + \alpha_0 \cos^2\theta_0 + \mathcal{P}_T \alpha_{BP}^+ \sin\theta_1 \sin\phi_1. \quad (8)$$

TABLE II. Summary of the systematic uncertainties. A , B , C and D stand for the modes of pK_S^0 , $\Lambda\pi^+$, $\Sigma^+\pi^0$, and $\Sigma^0\pi^+$, respectively.

Source	α_A^+	α_B^+	α_C^+	α_D^+	$\sin\Delta_0$	Δ_1^B	Δ_1^C	Δ_1^D
Reconstruction	0.00	0.00	0.00	0.01	0.00	0.8	0.0	0.0
$\pi^0\pi^0$ veto	0.01	0.00	0.01	0.00	0.00	0.0	0.2	0.0
ΔE signal region	0.07	0.01	0.02	0.05	0.02	0.3	0.1	0.1
M_{BC} signal region	0.12	0.01	0.05	0.02	0.02	0.5	0.4	0.1
Bkg subtraction	0.03	0.01	0.05	0.04	0.02	0.3	0.3	0.0
Total	0.14	0.02	0.07	0.07	0.03	1.0	0.6	0.2

Therefore, in a given $\cos\theta_0$ interval,

$$\langle \sin\theta_1 \sin\phi_1 \rangle = \frac{\int_0^{2\pi} \int_{-1}^1 \sin\theta_1 \sin\phi_1 \mathcal{W} d\cos\theta_1 d\phi_1}{\int_0^{2\pi} \int_{-1}^1 \mathcal{W} d\cos\theta_1 d\phi_1}$$

is directly proportional to $\alpha_{BP} P_T(\cos\theta_0)/(1 + \alpha_0 \cos^2\theta_0)$ for the acceptance corrected data. In Fig. 3(e), the effect of the transverse polarization $P_T(\cos\theta_0)$ is illustrated by plotting the average value $\langle \text{sign}(\alpha_{BP}) \sin\theta_1 \sin\phi_1 \rangle$ from all four decay modes and including both particles and antiparticles. The sign function of the measured decay asymmetry parameter, $\text{sign}(\alpha_{BP})$, is used to avoid the cancellation of contributions from the opposite charge modes.

The systematic uncertainties arise mainly from the reconstruction of final state tracks, $K_S^0 \rightarrow \pi^0\pi^0$ veto, ΔE requirement, signal M_{BC} selections and background subtraction. The contributions are summarized in Table II. The uncertainty of the input α_0 is found to be negligible, after considering the experimental uncertainty [27]. Systematic uncertainties from different sources are combined in quadrature to obtain the total systematic uncertainties.

To understand the reconstruction efficiencies in data and MC simulations, a series of control samples are used for different final states. The proton and charged pion are studied based on the channel $J/\psi \rightarrow p\bar{p}\pi^+\pi^-$, photon on $e^+e^- \rightarrow \gamma\mu^+\mu^-$ [34], π^0 on $\psi(3686) \rightarrow \pi^0\pi^0 J/\psi$ and $e^+e^- \rightarrow \omega\pi^0$, Λ on $J/\psi \rightarrow \bar{p}K^+\Lambda$ and $J/\psi \rightarrow \Lambda\bar{\Lambda}$ [35], and K_S^0 on $J/\psi \rightarrow K^*(892)^+K^-$, $K^*(892)^+ \rightarrow K_S^0\pi^+$ and $J/\psi \rightarrow \phi K_S^0 K^+\pi^-$ [36]. The efficiency differences between data and MC simulations are used to reweight

the summed likelihood values. The changes of the fit results after likelihood minimization are taken as systematic uncertainties. The uncertainties due to the $K_S^0 \rightarrow \pi^0\pi^0$ veto in $\Sigma^+\pi^0$ candidate events are evaluated by taking the maximum changes with respect to the nominal results when varying the $\pi^0\pi^0$ veto range. A similar method is applied when estimating the systematic uncertainties from the signal ΔE and M_{BC} selection criteria. In the likelihood construction, the subtraction of the background contributions are modeled with the sideband control samples and the inclusive MC samples. The associated uncertainties are studied by varying the sideband range and adjusting the scaling factors of the two background components. The altered scaling factors are obtained by changing the background lineshapes within their 1σ uncertainties from the fits to the M_{BC} distribution. The resultant maximum changes of the fit results are taken as corresponding systematic uncertainties.

To summarize, based on the 567 pb^{-1} data sample collected from e^+e^- collisions at a CM energy of 4.6 GeV, a simultaneous full angular analysis of four decay modes of $\Lambda_c^+ \rightarrow pK_S^0$, $\Lambda\pi^+$, $\Sigma^+\pi^0$, and $\Sigma^0\pi^+$ from the $e^+e^- \rightarrow \Lambda_c^+\Lambda_c^-$ production is carried out. We study the Λ_c^+ transverse polarization in unpolarized e^+e^- collisions for the first time, which gives $\sin\Delta_0 = -0.28 \pm 0.13 \pm 0.03$ with a statistical significance of 2.1σ . This information will help in understanding the production mechanism of the charmed baryons in e^+e^- annihilations. With availability of the transverse polarization measurement, the decay asymmetry parameter in $\Lambda_c^+ \rightarrow pK_S^0$ becomes accessible experimentally. Moreover, this improves the precision in determining the decay asymmetry parameters in $\Lambda_c^+ \rightarrow \Lambda\pi^+$, $\Sigma^+\pi^0$, and $\Sigma^0\pi^+$, as listed in Table I.

The parameters $\alpha_{pK_S^0}^+$ and $\alpha_{\Sigma^0\pi^+}^+$ are measured for the first time. The measured $\alpha_{\Lambda\pi^+}^+$ and $\alpha_{\Sigma^+\pi^0}^+$ parameters are consistent with previous measurements, but with much improved precisions (by a factor of 3 for $\alpha_{\Sigma^+\pi^0}^+$). The negative sign of the $\alpha_{\Sigma^+\pi^0}^+$ parameter is confirmed and differs from the positive predictions [10, 11, 16–19] by at least 8σ , which rules out those model calculations. The measured $\alpha_{\Sigma^+\pi^0}^+$ and $\alpha_{\Sigma^0\pi^+}^+$ values agree well, which

supports hyperon isospin symmetry in Λ_c^+ decay. For the results on $\alpha_{pK_S^0}^+$, $\alpha_{\Sigma^+\pi^0}^+$, and $\alpha_{\Sigma^0\pi^+}^+$ listed in Table I, at present no model gives predictions fully consistent with all the measurements. These improved results in Λ_c^+ decay asymmetries provide essential inputs for the b -baryon decay asymmetry measurements to be performed in the future.

The BESIII collaboration thanks the staff of BEPCII and the IHEP computing center for their strong support. This work is supported in part by National Key Basic Research Program of China under Contract No. 2015CB856700; National Natural Science Foundation of China (NSFC) under Contracts Nos. 11335008, 11425524, 11625523, 11635010, 11735014; the Chinese Academy of Sciences (CAS) Large-Scale Scientific Facility Program; the CAS Center for Excellence in Particle Physics (CCEPP); Joint Large-Scale Scientific Facility Funds of the NSFC and CAS under Contracts Nos. U1532257, U1532258, U1732263; CAS Key Research Program of Frontier Sciences under Contracts Nos. QYZDJ-SSW-SLH003, QYZDJ-SSW-SLH040; 100 Talents Program of CAS; INPAC and Shanghai Key Laboratory for Particle Physics and Cosmology; German Research Foundation DFG under Contract No. Collaborative Research Center CRC 1044, FOR 2359; Istituto Nazionale di Fisica Nucleare, Italy; Koninklijke Nederlandse Akademie van Wetenschappen (KNAW) under Contract No. 530-4CDP03; Ministry of Development of Turkey under Contract No. DPT2006K-120470; National Science and Technology fund; The Swedish Research Council; U. S. Department of Energy under Contracts Nos. DE-FG02-05ER41374, DE-SC-0010118, DE-SC-0012069; University of Groningen (RuG); Helmholtzzentrum fuer Schwerionenforschung GmbH (GSI), Darmstadt; the Knut and Alice Wallenberg Foundation (Sweden) under Contract No. 2016.0157 and the Royal Society, UK under Contract No. DH160214.

-
- [1] Y. Amhis *et al.* (HFLAV Collaboration), *Eur. Phys. J. C* **77**, 895 (2017).
[2] M. Tanabashi *et al.* (Particle Data Group), *Phys. Rev. D* **98**, 030001 (2018).
[3] C. D. Lü, W. Wang and F. S. Yu, *Phys. Rev. D* **93**, 056008 (2016).
[4] C. Q. Geng, Y. K. Hsiao, C. W. Liu and T. H. Tsai, *JHEP* **1711**, 147 (2017).
[5] F. S. Yu, H. Y. Jiang, R. H. Li, C. D. Lü, W. Wang and Z. X. Zhao, *Chin. Phys. C* **42**, 051001 (2018).
[6] R. Aaij *et al.* (LHCb Collaboration), *Phys. Rev. Lett.* **119**, 112001 (2017).
[7] H. Y. Cheng, *Front. Phys. (Beijing)* **10**, 101406 (2015).
[8] M. J. Savage and R. P. Springer, *Phys. Rev. D* **42**, 1527 (1990).
[9] J. D. Bjorken, *Phys. Rev. D* **40**, 1513 (1989).
[10] H. Y. Cheng and B. Tseng, *Phys. Rev. D* **48**, 4188 (1993).
[11] Q. P. Xu and A. N. Kamal, *Phys. Rev. D* **46**, 270 (1992).
[12] J. M. Link *et al.* (FOCUS Collaboration), *Phys. Lett. B* **634**, 165 (2006).
[13] M. Bishai *et al.* (CLEO Collaboration), *Phys. Lett. B* **350**, 256 (1995).
[14] H. Albrecht *et al.* (ARGUS Collaboration), *Phys. Lett. B* **274**, 239 (1992).
[15] P. Avery *et al.* (CLEO Collaboration), *Phys. Rev. Lett.* **65**, 2842 (1990).
[16] J. G. Korner and M. Kramer, *Z. Phys. C* **55**, 659 (1992).
[17] H. Y. Cheng and B. Tseng, *Phys. Rev. D* **46**, 1042 (1992);

- Erratum: [Phys. Rev. D **55**, 1697 (1997)].
- [18] M. A. Ivanov, J. G. Korner, V. E. Lyubovitskij, and A. G. Rusetsky, Phys. Rev. D **57**, 5632 (1998).
- [19] P. Zenczykowski, Phys. Rev. D **50**, 5787 (1994).
- [20] K. K. Sharma and R. C. Verma, Eur. Phys. J. C **7**, 217 (1999).
- [21] Y. Guan *et al.* (Belle Collaboration), Phys. Rev. Lett. **122**, 042001 (2019).
- [22] M. Ablikim *et al.* (BESIII Collaboration), arXiv:1808.08917 [hep-ex].
- [23] G. Fäldt, Phys. Rev. D **97**, 053002 (2018).
- [24] See Supplemental Material at [URL will be inserted by publisher] for the joint angular formula and Lee-Yang parameters.
- [25] M. Ablikim *et al.* (BESIII Collaboration), Phys. Rev. Lett. **116**, 052001 (2016).
- [26] H. Albrecht *et al.* (ARGUS Collaboration), Phys. Lett. B **241**, 278 (1990).
- [27] M. Ablikim *et al.* (BESIII Collaboration), Phys. Rev. Lett. **120**, 132001 (2018).
- [28] T. D. Lee and C. N. Yang, Phys. Rev. **104**, 254 (1956).
- [29] F. James and M. Roos, Comput. Phys. Commun. **10**, 343 (1975).
- [30] P. Zenczykowski, Phys. Rev. D **50**, 402 (1994).
- [31] A. Datta, hep-ph/9504428.
- [32] D. Wang, R.-G. Ping, L. Li, X.-R. Lyu, and Y.-H. Zheng, Chin. Phys. C **41**, 023106 (2017).
- [33] D. M. Asner *et al.*, Int. J. Mod. Phys. A **24**, S1 (2009).
- [34] V. Prasad, C. Liu, X. Ji, W. Li, H. Liu and X. Lou, Springer Proc. Phys. **174**, 577 (2016).
- [35] M. Ablikim *et al.* (BESIII Collaboration), Phys. Rev. Lett. **121**, 062003 (2018).
- [36] M. Ablikim *et al.* (BESIII Collaboration), Phys. Rev. D **92**, 112008 (2015).

1 Supplemental Material for "Measurements of Weak Decay Asymmetries of $\Lambda_c^+ \rightarrow pK_S^0$,
 2 $\Lambda\pi^+$, $\Sigma^+\pi^0$, and $\Sigma^0\pi^+$ "

3 M. Ablikim¹, M. N. Achasov^{10,d}, P. Adlarson⁵⁸, S. Ahmed¹⁵, M. Albrecht⁴, M. Alekseev^{57A,57C}, A. Amoroso^{57A,57C},
 4 F. F. An¹, Q. An^{54,42}, Y. Bai⁴¹, O. Bakina²⁷, R. Baldini Ferroli^{23A}, Y. Ban³⁵, K. Begzsuren²⁵, J. V. Bennett⁵, N. Berger²⁶,
 5 M. Bertani^{23A}, D. Bettoni^{24A}, F. Bianchi^{57A,57C}, J. Biernat⁵⁸, J. Bloms⁵¹, I. Boyko²⁷, R. A. Briere⁵, H. Cai⁵⁹, X. Cai^{1,42},
 6 A. Calcaterra^{23A}, G. F. Cao^{1,46}, N. Cao^{1,46}, S. A. Cetin^{45B}, J. Chai^{57C}, J. F. Chang^{1,42}, W. L. Chang^{1,46}, G. Chelkov^{27,b,c},
 7 D. Y. Chen⁶, G. Chen¹, H. S. Chen^{1,46}, J. C. Chen¹, M. L. Chen^{1,42}, S. J. Chen³³, Y. B. Chen^{1,42}, W. Cheng^{57C},
 8 G. Cibinetto^{24A}, F. Cossio^{57C}, X. F. Cui³⁴, H. L. Dai^{1,42}, J. P. Dai^{37,h}, X. C. Dai^{1,46}, A. Dbeysy¹⁵, D. Dedovich²⁷,
 9 Z. Y. Deng¹, A. Denig²⁶, I. Denysenko²⁷, M. Destefanis^{57A,57C}, F. De Mori^{57A,57C}, Y. Ding³¹, C. Dong³⁴, J. Dong^{1,42},
 10 L. Y. Dong^{1,46}, M. Y. Dong^{1,42,46}, Z. L. Dou³³, S. X. Du⁶², J. Z. Fan⁴⁴, J. Fang^{1,42}, S. S. Fang^{1,46}, Y. Fang¹,
 11 R. Farinelli^{24A,24B}, L. Fava^{57B,57C}, F. Feldbauer⁴, G. Felici^{23A}, C. Q. Feng^{54,42}, M. Fritsch⁴, C. D. Fu¹, Y. Fu¹, Q. Gao¹,
 12 X. L. Gao^{54,42}, Y. Gao⁵⁵, Y. Gao⁴⁴, Y. G. Gao⁶, Z. Gao^{54,42}, B. Garillon²⁶, I. Garzia^{24A}, E. M. Gersabeck⁴⁹, A. Gilman⁵⁰,
 13 K. Goetzen¹¹, L. Gong³⁴, W. X. Gong^{1,42}, W. Gradl²⁶, M. Greco^{57A,57C}, L. M. Gu³³, M. H. Gu^{1,42}, S. Gu Gu², Y. T. Gu¹³,
 14 A. Q. Guo²², L. B. Guo³², R. P. Guo^{1,46}, Y. P. Guo²⁶, A. Guskov²⁷, S. Han⁵⁹, X. Q. Hao¹⁶, F. A. Harris⁴⁷, K. L. He^{1,46},
 15 F. H. Heinsius⁴, T. Held⁴, Y. K. Heng^{1,42,46}, Y. R. Hou⁴⁶, Z. L. Hou¹, H. M. Hu^{1,46}, J. F. Hu^{37,h}, T. Hu^{1,42,46}, Y. Hu¹,
 16 G. S. Huang^{54,42}, J. S. Huang¹⁶, X. T. Huang³⁶, X. Z. Huang³³, Z. L. Huang³¹, N. Huesken⁵¹, T. Hussain⁵⁶, W. Ikegami⁵⁸,
 17 Andersson⁵⁸, W. Imoehl²², M. Irshad^{54,42}, Q. Ji¹, Q. P. Ji¹⁶, X. B. Ji^{1,46}, X. L. Ji^{1,42}, H. L. Jiang³⁶, X. S. Jiang^{1,42,46},
 18 X. Y. Jiang³⁴, J. B. Jiao³⁶, Z. Jiao¹⁸, D. P. Jin^{1,42,46}, S. Jin³³, Y. Jin⁴⁸, T. Johansson⁵⁸, N. Kalantar-Nayestanaki²⁹,
 19 X. S. Kang³¹, R. Kappert²⁹, M. Kavatsyuk²⁹, B. C. Ke¹, I. K. Keshk⁴, T. Khan^{54,42}, A. Khoukaz⁵¹, P. Kiese²⁶, R. Kiuchi¹,
 20 R. Kliebert¹¹, L. Koch²⁸, O. B. Kolcu^{45B,f}, B. Kopf⁴, M. Kuemmel⁴, M. Kuessner⁴, A. Kupsc⁵⁸, M. Kurth¹, M. G. Kurth^{1,46},
 21 W. Kühn²⁸, J. S. Lange²⁸, P. Larin¹⁵, L. Lavezzi^{57C}, H. Leithoff²⁶, T. Lenz²⁶, C. Li⁵⁸, Cheng Li^{54,42}, D. M. Li⁶², F. Li^{1,42},
 22 F. Y. Li³⁵, G. Li¹, H. B. Li^{1,46}, H. J. Li^{9,j}, J. C. Li¹, J. W. Li⁴⁰, K. Li¹, L. K. Li¹, Lei Li³, P. L. Li^{54,42}, P. R. Li³⁰,
 23 Q. Y. Li³⁶, W. D. Li^{1,46}, W. G. Li¹, X. H. Li^{54,42}, X. L. Li³⁶, X. N. Li^{1,42}, X. Q. Li³⁴, Z. B. Li⁴³, Z. Y. Li⁴³, H. Liang^{1,46},
 24 H. Liang^{54,42}, Y. F. Liang³⁹, Y. T. Liang²⁸, G. R. Liao¹², L. Z. Liao^{1,46}, J. Libby²¹, C. X. Lin⁴³, D. X. Lin¹⁵, Y. J. Lin¹³,
 25 B. Liu^{37,h}, B. J. Liu¹, C. X. Liu¹, D. Liu^{54,42}, D. Y. Liu^{37,h}, F. H. Liu³⁸, Fang Liu¹, Feng Liu⁶, H. B. Liu¹³, H. M. Liu^{1,46},
 26 Huanhuan Liu¹, Huihui Liu¹⁷, J. B. Liu^{54,42}, J. Y. Liu^{1,46}, K. Y. Liu³¹, Ke Liu⁶, Q. Liu⁴⁶, S. B. Liu^{54,42}, T. Liu^{1,46}, X. Liu³⁰,
 27 X. Y. Liu^{1,46}, Y. B. Liu³⁴, Z. A. Liu^{1,42,46}, Zhiqing Liu²⁶, Y. F. Long³⁵, X. C. Lou^{1,42,46}, H. J. Lu¹⁸, J. D. Lu^{1,46},
 28 J. G. Lu^{1,42}, Y. Lu¹, Y. P. Lu^{1,42}, C. L. Luo³², M. X. Luo⁶¹, P. W. Luo⁴³, T. Luo^{9,j}, X. L. Luo^{1,42}, S. Lusso^{57C}, X. R. Lyu⁴⁶,
 29 F. C. Ma³¹, H. L. Ma¹, L. L. Ma³⁶, M. M. Ma^{1,46}, Q. M. Ma¹, X. N. Ma³⁴, X. X. Ma^{1,46}, X. Y. Ma^{1,42}, Y. M. Ma³⁶,
 30 F. E. Maas¹⁵, M. Maggiora^{57A,57C}, S. Maldaner²⁶, S. Malde⁵², Q. A. Malik⁵⁶, A. Mangoni^{23B}, Y. J. Mao³⁵, Z. P. Mao¹,
 31 S. Marcellò^{57A,57C}, Z. X. Meng⁴⁸, J. G. Messchendorp²⁹, G. Mezzadri^{24A}, J. Min^{1,42}, T. J. Min³³, R. E. Mitchell²²,
 32 X. H. Mo^{1,42,46}, Y. J. Mo⁶, C. Morales Morales¹⁵, N. Yu. Muchnoi^{10,d}, H. Muramatsu⁵⁰, A. Mustafa⁴, S. Nakhoul^{11,g},
 33 Y. Nefedov²⁷, F. Nerling^{11,g}, I. B. Nikolaev^{10,d}, Z. Ning^{1,42}, S. Nisar^{38,k}, S. L. Niu^{1,42}, S. L. Olsen⁴⁶, Q. Ouyang^{1,42,46},
 34 S. Pacetti^{23B}, Y. Pan^{54,42}, M. Papenbrock⁵⁸, P. Patteri^{23A}, M. Pelizaeus⁴, H. P. Peng^{54,42}, K. Peters^{11,g}, J. Pettersson⁵⁸,
 35 J. L. Ping³², R. G. Ping^{1,46}, A. Pitka⁴, R. Poling⁵⁰, V. Prasad^{54,42}, M. Q³³, T. Y. Qi², S. Qian^{1,42}, C. F. Qiao⁴⁶, N. Qin⁵⁹,
 36 X. P. Qin¹³, X. S. Qin⁴, Z. H. Qin^{1,42}, J. F. Qiu⁴, S. Q. Qu³⁴, K. H. Rashid^{56,i}, C. F. Redmer²⁶, M. Richter⁴, M. Ripka²⁶,
 37 A. Rivetti^{57C}, V. Rodin²⁹, M. Rolo^{57C}, G. Rong^{1,46}, Ch. Rosner¹⁵, M. Rump⁵¹, A. Sarantsev^{27,e}, M. Savrić^{24B},
 38 K. Schoenning⁵⁸, W. Shan¹⁹, X. Y. Shan^{54,42}, M. Shao^{54,42}, C. P. Shen², P. X. Shen³⁴, X. Y. Shen^{1,46}, H. Y. Sheng¹,
 39 X. Shi^{1,42}, X. D. Shi^{54,42}, J. J. Song³⁶, Q. Q. Song^{54,42}, X. Y. Song¹, S. Sosio^{57A,57C}, C. Sowa⁴, S. Spataro^{57A,57C}, F. F.
 40 Sui³⁶, G. X. Sun¹, J. F. Sun¹⁶, L. Sun⁵⁹, S. S. Sun^{1,46}, X. H. Sun¹, Y. J. Sun^{54,42}, Y. K. Sun^{54,42}, Y. Z. Sun¹, Z. J. Sun^{1,42},
 41 Z. T. Sun¹, Y. T. Tan^{54,42}, C. J. Tang³⁹, G. Y. Tang¹, X. Tang¹, V. Thoren⁵⁸, B. Tsednee²⁵, I. Uman^{45D}, B. Wang¹,
 42 B. L. Wang⁴⁶, C. W. Wang³³, D. Y. Wang³⁵, H. H. Wang³⁶, K. Wang^{1,42}, L. L. Wang¹, L. S. Wang¹, M. Wang³⁶,
 43 M. Z. Wang³⁵, Meng Wang^{1,46}, P. L. Wang¹, R. M. Wang⁶⁰, W. P. Wang^{54,42}, X. Wang³⁵, X. F. Wang¹, X. L. Wang^{9,j},
 44 Y. Wang^{54,42}, Y. Wang⁴³, Y. F. Wang^{1,42,46}, Z. Wang^{1,42}, Z. G. Wang^{1,42}, Z. Y. Wang¹, Zongyuan Wang^{1,46}, T. Weber⁴,
 45 D. H. Wei¹², P. Weidenkaff²⁶, H. W. Wen³², S. P. Wen¹, U. Wiedner⁴, G. Wilkinson⁵², M. Wolke⁵⁸, L. H. Wu¹,
 46 L. J. Wu^{1,46}, Z. Wu^{1,42}, L. Xia^{54,42}, Y. Xia²⁰, S. Y. Xiao¹, Y. J. Xiao^{1,46}, Z. J. Xiao³², Y. G. Xie^{1,42}, Y. H. Xie⁶,
 47 T. Y. Xing^{1,46}, X. A. Xiong^{1,46}, Q. L. Xiu^{1,42}, G. F. Xu¹, L. Xu¹, Q. J. Xu¹⁴, W. Xu^{1,46}, X. P. Xu⁴⁰, F. Yan⁵⁵,
 48 L. Yan^{57A,57C}, W. B. Yan^{54,42}, W. C. Yan², Y. H. Yan²⁰, H. J. Yang^{37,h}, H. X. Yang¹, L. Yang⁵⁹, R. X. Yang^{54,42},
 49 S. L. Yang^{1,46}, Y. H. Yang³³, Y. X. Yang¹², Yifan Yang^{1,46}, Z. Q. Yang³⁰, M. Ye^{1,42}, M. H. Ye⁷, J. H. Yin¹, Z. Y. You⁴³,
 50 B. X. Yu^{1,42,46}, C. X. Yu³⁴, J. S. Yu²⁰, C. Z. Yuan^{1,46}, X. Q. Yuan³⁵, Y. Yuan¹, A. Yuncu^{45B,a}, A. A. Zafar⁵⁶, Y. Zeng²⁰,
 51 B. X. Zhang¹, B. Y. Zhang^{1,42}, C. C. Zhang¹, D. H. Zhang¹, H. H. Zhang⁴³, H. Y. Zhang^{1,42}, J. Zhang^{1,46}, J. L. Zhang⁶⁰,
 52 J. Q. Zhang⁴, J. W. Zhang^{1,42,46}, J. Y. Zhang¹, J. Z. Zhang^{1,46}, K. Zhang^{1,46}, L. Zhang⁴⁴, S. F. Zhang³³, T. J. Zhang^{37,h},
 53 X. Y. Zhang³⁶, Y. Zhang^{54,42}, Y. H. Zhang^{1,42}, Y. T. Zhang^{54,42}, Yang Zhang¹, Yao Zhang¹, Yi Zhang^{9,j}, Yu Zhang⁴⁶,
 54 Z. H. Zhang⁶, Z. P. Zhang⁵⁴, Z. Y. Zhang⁵⁹, G. Zhao¹, J. W. Zhao^{1,42}, J. Y. Zhao^{1,46}, J. Z. Zhao^{1,42}, Lei Zhao^{54,42},
 55 Ling Zhao¹, M. G. Zhao³⁴, Q. Zhao¹, S. J. Zhao⁶², T. C. Zhao¹, Y. B. Zhao^{1,42}, Z. G. Zhao^{54,42}, A. Zhemchugov^{27,b},
 56 B. Zheng⁵⁵, J. P. Zheng^{1,42}, Y. Zheng³⁵, Y. H. Zheng⁴⁶, B. Zhong³², L. Zhou^{1,42}, L. P. Zhou^{1,46}, Q. Zhou^{1,46}, X. Zhou⁵⁹,
 57 X. K. Zhou⁴⁶, X. R. Zhou^{54,42}, Xiaoyu Zhou²⁰, Xu Zhou²⁰, A. N. Zhu^{1,46}, J. Zhu³⁴, J. Zhu⁴³, K. J. Zhu^{1,42,46},
 58 S. H. Zhu⁵³, W. J. Zhu³⁴, X. L. Zhu⁴⁴, Y. C. Zhu^{54,42}, Y. S. Zhu^{1,46}, Z. A. Zhu^{1,46}, J. Zhuang^{1,42}, B. S. Zou¹, J. H. Zou¹

(BESIII Collaboration)

¹ Institute of High Energy Physics, Beijing 100049, People's Republic of China

² Beihang University, Beijing 100191, People's Republic of China

- 62 ³ Beijing Institute of Petrochemical Technology, Beijing 102617, People's Republic of China
63 ⁴ Bochum Ruhr-University, D-44780 Bochum, Germany
64 ⁵ Carnegie Mellon University, Pittsburgh, Pennsylvania 15213, USA
65 ⁶ Central China Normal University, Wuhan 430079, People's Republic of China
66 ⁷ China Center of Advanced Science and Technology, Beijing 100190, People's Republic of China
67 ⁸ COMSATS University Islamabad, Lahore Campus, Defence Road, Off Raiwind Road, 54000 Lahore, Pakistan
68 ⁹ Fudan University, Shanghai 200443, People's Republic of China
69 ¹⁰ G.I. Budker Institute of Nuclear Physics SB RAS (BINP), Novosibirsk 630090, Russia
70 ¹¹ GSI Helmholtzcentre for Heavy Ion Research GmbH, D-64291 Darmstadt, Germany
71 ¹² Guangxi Normal University, Guilin 541004, People's Republic of China
72 ¹³ Guangxi University, Nanning 530004, People's Republic of China
73 ¹⁴ Hangzhou Normal University, Hangzhou 310036, People's Republic of China
74 ¹⁵ Helmholtz Institute Mainz, Johann-Joachim-Becher-Weg 45, D-55099 Mainz, Germany
75 ¹⁶ Henan Normal University, Xinxiang 453007, People's Republic of China
76 ¹⁷ Henan University of Science and Technology, Luoyang 471003, People's Republic of China
77 ¹⁸ Huangshan College, Huangshan 245000, People's Republic of China
78 ¹⁹ Hunan Normal University, Changsha 410081, People's Republic of China
79 ²⁰ Hunan University, Changsha 410082, People's Republic of China
80 ²¹ Indian Institute of Technology Madras, Chennai 600036, India
81 ²² Indiana University, Bloomington, Indiana 47405, USA
82 ²³ (A)INFN Laboratori Nazionali di Frascati, I-00044, Frascati,
83 Italy; (B)INFN and University of Perugia, I-06100, Perugia, Italy
84 ²⁴ (A)INFN Sezione di Ferrara, I-44122, Ferrara, Italy; (B)University of Ferrara, I-44122, Ferrara, Italy
85 ²⁵ Institute of Physics and Technology, Peace Ave. 54B, Ulaanbaatar 13330, Mongolia
86 ²⁶ Johannes Gutenberg University of Mainz, Johann-Joachim-Becher-Weg 45, D-55099 Mainz, Germany
87 ²⁷ Joint Institute for Nuclear Research, 141980 Dubna, Moscow region, Russia
88 ²⁸ Justus-Liebig-Universitaet Giessen, II. Physikalisches Institut, Heinrich-Buff-Ring 16, D-35392 Giessen, Germany
89 ²⁹ KVI-CART, University of Groningen, NL-9747 AA Groningen, The Netherlands
90 ³⁰ Lanzhou University, Lanzhou 730000, People's Republic of China
91 ³¹ Liaoning University, Shenyang 110036, People's Republic of China
92 ³² Nanjing Normal University, Nanjing 210023, People's Republic of China
93 ³³ Nanjing University, Nanjing 210093, People's Republic of China
94 ³⁴ Nankai University, Tianjin 300071, People's Republic of China
95 ³⁵ Peking University, Beijing 100871, People's Republic of China
96 ³⁶ Shandong University, Jinan 250100, People's Republic of China
97 ³⁷ Shanghai Jiao Tong University, Shanghai 200240, People's Republic of China
98 ³⁸ Shanxi University, Taiyuan 030006, People's Republic of China
99 ³⁹ Sichuan University, Chengdu 610064, People's Republic of China
100 ⁴⁰ Soochow University, Suzhou 215006, People's Republic of China
101 ⁴¹ Southeast University, Nanjing 211100, People's Republic of China
102 ⁴² State Key Laboratory of Particle Detection and Electronics, Beijing 100049, Hefei 230026, People's Republic of China
103 ⁴³ Sun Yat-Sen University, Guangzhou 510275, People's Republic of China
104 ⁴⁴ Tsinghua University, Beijing 100084, People's Republic of China
105 ⁴⁵ (A)Ankara University, 06100 Tandogan, Ankara, Turkey; (B)Istanbul Bilgi University, 34060 Eyup, Istanbul, Turkey;
106 (C)Uludag University, 16059 Bursa, Turkey; (D)Near East University, Nicosia, North Cyprus, Mersin 10, Turkey
107 ⁴⁶ University of Chinese Academy of Sciences, Beijing 100049, People's Republic of China
108 ⁴⁷ University of Hawaii, Honolulu, Hawaii 96822, USA
109 ⁴⁸ University of Jinan, Jinan 250022, People's Republic of China
110 ⁴⁹ University of Manchester, Oxford Road, Manchester, M13 9PL, United Kingdom
111 ⁵⁰ University of Minnesota, Minneapolis, Minnesota 55455, USA
112 ⁵¹ University of Muenster, Wilhelm-Klemm-Str. 9, 48149 Muenster, Germany
113 ⁵² University of Oxford, Keble Rd, Oxford, UK OX13RH
114 ⁵³ University of Science and Technology Liaoning, Anshan 114051, People's Republic of China
115 ⁵⁴ University of Science and Technology of China, Hefei 230026, People's Republic of China
116 ⁵⁵ University of South China, Hengyang 421001, People's Republic of China
117 ⁵⁶ University of the Punjab, Lahore-54590, Pakistan
118 ⁵⁷ (A)University of Turin, I-10125, Turin, Italy; (B)University of Eastern
119 Piedmont, I-15121, Alessandria, Italy; (C)INFN, I-10125, Turin, Italy
120 ⁵⁸ Uppsala University, Box 516, SE-75120 Uppsala, Sweden
121 ⁵⁹ Wuhan University, Wuhan 430072, People's Republic of China
122 ⁶⁰ Xinyang Normal University, Xinyang 464000, People's Republic of China
123 ⁶¹ Zhejiang University, Hangzhou 310027, People's Republic of China
124 ⁶² Zhengzhou University, Zhengzhou 450001, People's Republic of China

125
126
127
128
129
130
131
132
133
134
135
136
137
138

^a Also at Bogazici University, 34342 Istanbul, Turkey

^b Also at the Moscow Institute of Physics and Technology, Moscow 141700, Russia

^c Also at the Functional Electronics Laboratory, Tomsk State University, Tomsk, 634050, Russia

^d Also at the Novosibirsk State University, Novosibirsk, 630090, Russia

^e Also at the NRC "Kurchatov Institute", PNPI, 188300, Gatchina, Russia

^f Also at Istanbul Arel University, 34295 Istanbul, Turkey

^g Also at Goethe University Frankfurt, 60323 Frankfurt am Main, Germany

^h Also at Key Laboratory for Particle Physics, Astrophysics and Cosmology, Ministry of Education; Shanghai Key Laboratory for Particle Physics and Cosmology; Institute of Nuclear and Particle Physics, Shanghai 200240, People's Republic of China

ⁱ Also at Government College Women University, Sialkot - 51310. Punjab, Pakistan.

^j Also at Key Laboratory of Nuclear Physics and Ion-beam Application (MOE) and Institute of Modern Physics, Fudan University, Shanghai 200443, People's Republic of China

^k Also at Harvard University, Department of Physics, Cambridge, MA, 02138, USA

(Dated: April 30, 2019)

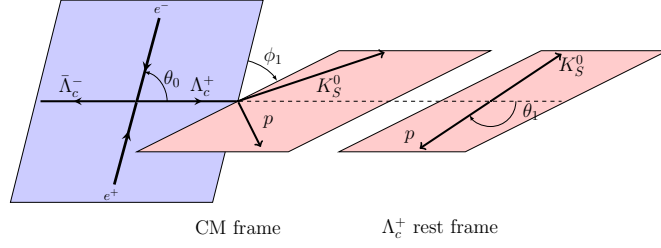


FIG. 1. Definition of the helicity frames for $e^+e^- \rightarrow \Lambda_c^+\bar{\Lambda}_c^-$, $\Lambda_c^+ \rightarrow pK_S^0$

139 For the process $e^+e^- \rightarrow \Lambda_c^+\bar{\Lambda}_c^-$, $\Lambda_c^+ \rightarrow BP$ and $\bar{\Lambda}_c^- \rightarrow$ inclusive, where B and P denote a $J^P = \frac{1}{2}^+$ baryon and a
 140 pseudoscalar meson, respectively, the amplitude can be constructed under the helicity basis. For the weak non-leptonic
 141 decay $\Lambda_c^+ \rightarrow BP$, the Lee-Yang variables[1] α_{BP} , β_{BP} , and γ_{BP} are defined with respect to the s -wave and p -wave
 142 amplitudes, such as

$$\alpha_{BP} = \frac{2\text{Re}(s \cdot p)}{|s|^2 + |p|^2}, \quad \beta_{BP} = \frac{2\text{Im}(s \cdot p)}{|s|^2 + |p|^2}, \quad \gamma_{BP} = \frac{|s|^2 - |p|^2}{|s|^2 + |p|^2}, \quad (1)$$

143 and with equality $\alpha_{BP}^2 + \beta_{BP}^2 + \gamma_{BP}^2 = 1$.

144 We work with helicity amplitudes. For $\Lambda_c^+ \rightarrow B(\frac{1}{2}^+)P(0^-)$ decay, we have two helicity amplitudes, $H_{1/2}$ and
 145 $H_{-1/2}$. Using relations $s = \frac{1}{\sqrt{2}}(H_{1/2} + H_{-1/2})$, $p = \frac{1}{\sqrt{2}}(H_{1/2} - H_{-1/2})$, we have the asymmetry parameters defined
 146 with helicity amplitudes as

$$\alpha_{BP} = |H_{1/2}|^2 - |H_{-1/2}|^2, \quad \beta_{BP} = \sqrt{1 - \alpha_{BP}^2} \sin \Delta_1^{BP}, \quad \gamma_{BP} = \sqrt{1 - \alpha_{BP}^2} \cos \Delta_1^{BP}, \quad (2)$$

147 here we have taken the normalization $|H_{1/2}|^2 + |H_{-1/2}|^2 = 1$, and Δ_1^{BP} is the phase angle difference between two
 148 helicity amplitudes $H_{1/2}$ and $H_{-1/2}$.

149 If Λ_c^+ and $\bar{\Lambda}_c^-$ decays conserve the CP transformation, we have relations for the $\bar{\Lambda}_c^-$ asymmetry parameters as

$$\bar{\alpha}_{BP} = -\alpha_{BP}, \quad \bar{\beta}_{BP} = -\beta_{BP}, \quad \bar{\gamma}_{BP} = \gamma_{BP}. \quad (3)$$

150 In the context, for the helicity frame of Λ_c^+ production process $e^+e^- \rightarrow \Lambda_c^+\bar{\Lambda}_c^-$, θ_0 is defined as the polar angle of
 151 the Λ_c^+ with respect to the e^+ beam axis in the e^+e^- center-of mass (CM) system, as illustrated in Fig. 1.

152 I. JOINT ANGULAR DISTRIBUTION FOR THE DECAY $\Lambda_c^+ \rightarrow pK_S^0$

153 Figure 1 illustrates the definitions of the helicity angles for a 1-level decay $\Lambda_c^+ \rightarrow pK_S^0$. In the helicity system
 154 describing the $\Lambda_c^+ \rightarrow pK_S^0$ decay, the angle ϕ_1 is the angle between the $e^+\Lambda_c^+$ plane and pK_S^0 plane, and θ_1 is the
 155 polar angle of the p momentum in the rest frame of the Λ_c^+ with respect to the Λ_c^+ momentum in the CM frame.

TABLE I. Definition of decays, helicity angles and amplitudes of $\Lambda_c^+ \rightarrow pK_S^0$, where λ_i indicates the helicity for the corresponding hadron.

level	reaction	helicity angle	helicity amplitude
0	$e^+e^- \rightarrow \gamma^* \rightarrow \Lambda_c^+(\lambda_1)\bar{\Lambda}_c^-(\lambda_2)$	θ_0	A_{λ_1,λ_2}
1	$\Lambda_c^+ \rightarrow p(\lambda_3)K_S^0$	(θ_1, ϕ_1)	B_{λ_3}

156 As listed in Table I, λ_1 , λ_2 , and λ_3 denote the helicities of Λ_c^+ , $\bar{\Lambda}_c^-$ and p . A_{λ_1,λ_2} and B_{λ_3} are the helicity amplitudes.
 157 The differential decay rate is defined as

$$M_{\lambda_i} = D_{m,\lambda_1-\lambda_2}^1(\theta_0)A_{\lambda_1,\lambda_2}D_{\lambda_1,\lambda_3}^{\frac{1}{2}}(\Omega_i)B_{\lambda_3}, \quad (4)$$

TABLE II. Definition of decays, helicity angles and amplitudes in $\Lambda_c^+ \rightarrow \Lambda\pi^+$, where λ_i indicates the helicity values for the corresponding hadron.

level	reaction	helicity angle	helicity amplitude
0	$e^+e^- \rightarrow \gamma^* \rightarrow \Lambda_c^+(\lambda_1)\Lambda_c^-(\lambda_2)$	θ_0	A_{λ_1,λ_2}
1	$\Lambda_c^+ \rightarrow \Lambda(\lambda_3)\pi^+$	(θ_1, ϕ_1)	B_{λ_3}
2	$\Lambda \rightarrow p(\lambda_4)\pi^-$	(θ_2, ϕ_2)	C_{λ_4}

158 where m is the helicity of virtual photon, $D_{m,\lambda_1-\lambda_2}^1(\theta_0)$ and $D_{\lambda_1,\lambda_2}^{\frac{1}{2}}(\Omega_i) \equiv D_{\lambda_1,\lambda_2}^{\frac{1}{2}}(\phi_i, \theta_i, 0)$ is Wigner-D function [2].
 159 The total helicity amplitudes is calculated by

$$|M|^2 = \sum_m \left| \sum_{\lambda_i} M_{\lambda_i} \right|^2 = \sum_m \left(\sum_{\lambda_i} M \right) \left(\sum_{\lambda'_j} M^* \right). \quad (5)$$

160 If we define the γ^* spin density matrix $\rho^{(\lambda_1-\lambda_2, \lambda'_1-\lambda_2)} = \sum_{m=\pm 1} d_{m,\lambda_1-\lambda_2}^1(\theta_0) d_{m,\lambda'_1-\lambda_2}^1(\theta_0)$ we can get

$$\begin{aligned} \frac{d\Gamma}{d \cos \theta_0 d \cos \theta_1 d \phi_1} &\propto \sum_{m,\lambda_1,\lambda_2,\lambda_3} D_{m,\lambda_1-\lambda_2}^{1*}(0, \theta_0, 0) D_{m,\lambda'_1-\lambda_2}^1(0, \theta_0, 0) A_{\lambda_1,\lambda_2}^* A_{\lambda'_1,\lambda_2} \\ &\times D_{\lambda_1,\lambda_3}^{1/2*}(\phi_1, \theta_1, 0) D_{\lambda'_1,\lambda_3}^{1/2}(\phi_1, \theta_1, 0) |B_{\lambda_3}|^2, \end{aligned} \quad (6)$$

161 Helicity amplitude A_{λ_1,λ_2} is related to the angular distribution parameters $\alpha_0 = \frac{|A_{\frac{1}{2},-\frac{1}{2}}|^2 - 2|A_{\frac{1}{2},\frac{1}{2}}|^2}{|A_{\frac{1}{2},-\frac{1}{2}}|^2 + 2|A_{\frac{1}{2},\frac{1}{2}}|^2}$, and helicity
 162 amplitude B_{λ_3} is related to the decay asymmetry parameter $\alpha_{pK_S^0}^+ = \frac{|B_{\frac{1}{2}}|^2 - |B_{-\frac{1}{2}}|^2}{|B_{\frac{1}{2}}|^2 + |B_{-\frac{1}{2}}|^2}$. In helicity frame, conventional
 163 s -wave amplitude can be expressed by $\frac{1}{\sqrt{2}}(B_{\frac{1}{2}} + B_{-\frac{1}{2}})$ and p -wave by $\frac{1}{\sqrt{2}}(B_{\frac{1}{2}} - B_{-\frac{1}{2}})$. The joint angular dependence
 164 of the decay rate is written as

$$\frac{d\Gamma}{d \cos \theta_0 d \cos \theta_1 d \phi_1} \propto 1 + \alpha_0 \cos^2 \theta_0 + \mathcal{P}_T \alpha_{pK_S^0}^+ \sin \theta_1 \sin \phi_1, \quad (7)$$

$$\mathcal{P}_T = \sqrt{1 - \alpha_0^2} \cos \theta_0 \sin \theta_0 \sin \Delta_0, \quad (8)$$

165 where $\Delta_0 = \delta_{\frac{1}{2},\frac{1}{2}} - \delta_{\frac{1}{2},-\frac{1}{2}}$ is the difference of phase angle for the helicity amplitudes $A_{\frac{1}{2},\frac{1}{2}}$ and $A_{\frac{1}{2},-\frac{1}{2}}$, and \mathcal{P}_T
 166 corresponds to a transverse polarization observable of the produced Λ_c^+ . For the charge conjugation mode $\Lambda_c^- \rightarrow \bar{p}K_S^0$,
 167 the formula of angular distribution is same, but with the parameter relations of $\bar{\Delta}_0 = \Delta_0$ and $\bar{\alpha}_{\bar{p}K_S^0}^- = -\alpha_{pK_S^0}^+$, when
 168 neglecting CP violation.

169 II. JOINT ANGULAR DISTRIBUTION FOR THE DECAYS $\Lambda_c^+ \rightarrow \Lambda\pi^+$ AND $\Sigma^+\pi^0$

170 Figure 2 illustrates the definitions of the helicity angles for a 2-level cascade decay $\Lambda_c^+ \rightarrow \Lambda\pi^+$, $\Lambda \rightarrow p\pi^-$. In the
 171 helicity system describing the $\Lambda_c^+ \rightarrow \Lambda\pi^+$ decay, the angle ϕ_1 is the angle between the $e^+\Lambda_c^+$ plane and $\Lambda\pi^+$ plane,
 172 and θ_1 is the polar angle of the Λ momentum in the rest frame of the Λ_c^+ with respect to the Λ_c^+ momentum in the
 173 CM frame. In the the helicity system describing the $\Lambda \rightarrow p\pi^-$ decay, the angle ϕ_2 is the angle between the $\Lambda\pi^+$
 174 plane and $p\pi^-$ plane, and θ_2 is the polar angle of the proton momentum with respect to the opposite direction of π^+
 175 momentum in the rest frame of Λ .

176 As listed in Table II, B_{λ_3} and C_{λ_4} are the helicity amplitudes of the $\Lambda_c^+ \rightarrow \Lambda\pi^+$ and $\Lambda \rightarrow p\pi^-$ decays, respectively.

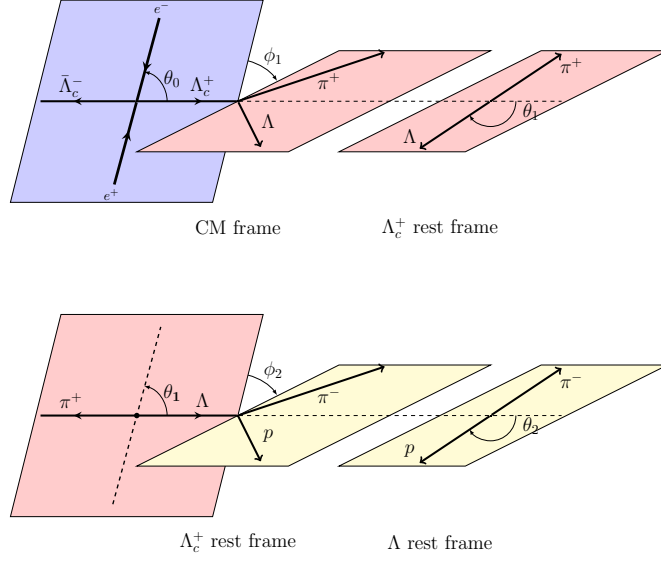


FIG. 2. Definition of the helicity frame for $e^+e^- \rightarrow \Lambda_c^+ \bar{\Lambda}_c^-$, $\Lambda_c^+ \rightarrow \Lambda \pi^+$ and $\Lambda \rightarrow p \pi^-$

177 The joint angular dependence of the decay rate is written as

$$\begin{aligned}
 & \frac{d\Gamma}{d \cos \theta_0 d \cos \theta_1 d \cos \theta_2 d \phi_1 d \phi_2} \\
 & \propto 2 + 2\alpha_0 \cos^2 \theta_0 \\
 & + \sqrt{1 - \alpha_0^2} \alpha_\Lambda \sin \Delta_0 \sin(2\theta_0) \sin \theta_1 \cos \theta_2 \sin \phi_1 \\
 & + \sqrt{1 - \alpha_0^2} \alpha_\Lambda \sin \Delta_0 \sin(2\theta_0) \cos \theta_1 \sin \theta_2 \sin \phi_1 \sqrt{1 - (\alpha_{\Lambda\pi^+}^+)^2} \cos(\Delta_1^{\Lambda\pi^+} + \phi_2) \\
 & + \sqrt{1 - \alpha_0^2} \alpha_\Lambda \sin \Delta_0 \sin(2\theta_0) \sin \theta_2 \cos \phi_1 \sqrt{1 - (\alpha_{\Lambda\pi^+}^+)^2} \sin(\Delta_1^{\Lambda\pi^+} + \phi_2) \\
 & + \sqrt{1 - \alpha_0^2} \sin \Delta_0 \sin(2\theta_0) \sin \theta_1 \sin \phi_1 \alpha_{\Lambda\pi^+}^+ \\
 & + 2\alpha_0 \alpha_\Lambda \cos^2 \theta_0 \cos \theta_2 \alpha_{\Lambda\pi^+}^+ + 2\alpha_\Lambda \cos \theta_2 \alpha_{\Lambda\pi^+}^+,
 \end{aligned} \tag{9}$$

178 where α_Λ denotes the decay asymmetry parameter in the weak hadronic decay $\Lambda \rightarrow p \pi^-$, $\Delta_0 = \delta_{\frac{1}{2}, -\frac{1}{2}} - \delta_{\frac{1}{2}, \frac{1}{2}}$ is the
 179 difference of phase angle for the helicity amplitudes A_{λ_1, λ_2} and $\Delta_1^{\Lambda\pi^+}$ is the difference of the phase angle between the
 180 helicity amplitudes $B_{-\frac{1}{2}}$ and $B_{\frac{1}{2}}$. For the case of the charge conjugation mode $\bar{\Lambda}_c^- \rightarrow \bar{\Lambda} \pi^-$, the formula is the same,
 181 but with the parameter relations of $\bar{\alpha}_{\bar{\Lambda}} = -\alpha_\Lambda$, $\bar{\alpha}_{\bar{\Lambda}\pi^-} = -\alpha_{\Lambda\pi^+}^+$, $\bar{\Delta}_0 = \Delta_0$, $\bar{\Delta}_1^{\bar{\Lambda}\pi^-} = -\Delta_1^{\Lambda\pi^+}$ on the basis of no CP
 182 violation.

183 If the phase space of level-2 decay $\Omega_2 = (\theta_2, \phi_2)$ is integrated out, one has

$$\frac{d\Gamma}{d \cos \theta_0 d \cos \theta_1 d \phi_1} \propto 1 + \alpha_0 \cos^2 \theta_0 + \mathcal{P}_T \alpha_{\Lambda\pi^+}^+ \sin \theta_1 \sin \phi_1, \tag{10}$$

$$\mathcal{P}_T = \sqrt{1 - \alpha_0^2} \cos \theta_0 \sin \theta_0 \sin \Delta_0. \tag{11}$$

184 Equation (7) becomes in the same form of Eq. (4). If the proton helicity angular θ_2 is only measured, one has

$$\frac{dN}{d \cos \theta_2} \propto 1 + \alpha_{\Lambda\pi^+}^+ \alpha_\Lambda \cos \theta_2. \tag{12}$$

185 This equation indicates that even without information of \mathcal{P}_T , the decay asymmetry parameter $\alpha_{\Lambda\pi^+}^+$ can be accessed
 186 from the distribution of $\cos \theta_2$.

TABLE III. Definition of decays, helicity angles and amplitudes in $\Lambda_c^+ \rightarrow \Sigma^+ \pi^0$, where λ_i indicates the helicity values for the corresponding hadron.

level	reaction	helicity angle	helicity amplitude
0	$e^+ e^- \rightarrow \gamma^* \rightarrow \Lambda_c^+(\lambda_1) \bar{\Lambda}_c^-(\lambda_2)$	θ_0	A_{λ_1, λ_2}
1	$\Lambda_c^+ \rightarrow \Sigma^+(\lambda_3) \pi^0$	(θ_1, ϕ_1)	B_{λ_3}
2	$\Sigma^+ \rightarrow p(\lambda_4) \pi^0$	(θ_2, ϕ_2)	C_{λ_4}

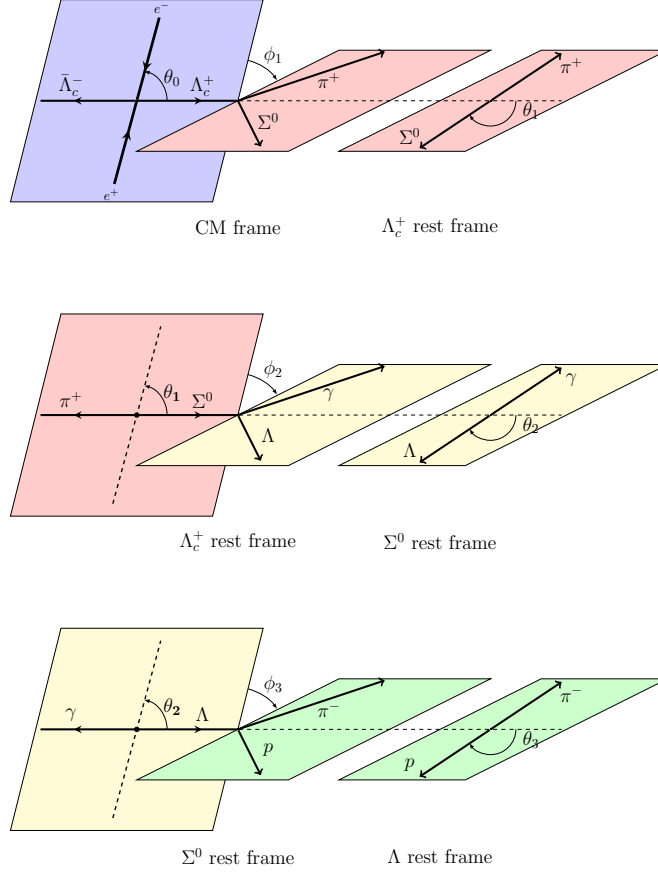


FIG. 3. Definition of the helicity frame for $e^+ e^- \rightarrow \Lambda_c^+ \bar{\Lambda}_c^-$, $\Lambda_c^+ \rightarrow \Sigma^0 \pi^+$, $\Sigma^0 \rightarrow \gamma \Lambda$, $\Lambda \rightarrow p \pi^-$.

187 For the 2-level cascade decays $\Lambda_c^+ \rightarrow \Sigma^+ \pi^0$, $\Sigma^+ \rightarrow p \pi^0$, the formalism is the analogous to that of $\Lambda_c^+ \rightarrow \Lambda \pi^+$ as
 188 listed in Table III, but replacing the symbols of Λ and π^+ with Σ^+ and π^0 in the level-1 decay and replacing π^- with
 189 π^0 in the level-2 decay, respectively.

190 III. JOINT ANGULAR DISTRIBUTION FOR $\Lambda_c^+ \rightarrow \Sigma^0 \pi^+$

191 Figure 3 illustrates the definitions of the helicity angles for a 3-level cascade decay $\Lambda_c^+ \rightarrow \Sigma^0 \pi^+$, $\Sigma^0 \rightarrow \gamma \Lambda$, $\Lambda \rightarrow p \pi^-$.
 192 In the helicity system describing the $\Lambda_c^+ \rightarrow \Sigma^0 \pi^+$ decay, the angle ϕ_1 is the angle between the $e^+ \Lambda_c^+$ plane and $\Sigma^0 \pi^+$
 193 plane, and θ_1 is the polar angle of the Σ^0 momentum in the rest frame of the Λ_c^+ with respect to the Λ_c^+ momentum in
 194 the CM frame. In the helicity system describing the $\Sigma^0 \rightarrow \gamma \Lambda$ decay, the angle ϕ_2 is the angle between the $\Sigma^0 \pi^+$ plane
 195 and $\gamma \Lambda$ plane, and θ_2 is the polar angle of the Λ momentum with respect to the opposite direction of π^+ momentum
 196 in the rest frame of Σ^0 . In the helicity system describing the $\Lambda \rightarrow p \pi^-$ process, ϕ_3 is the angle between the $\Lambda \gamma$ and

TABLE IV. Definition of decays, helicity angles and amplitudes in $\Lambda_c^+ \rightarrow \Sigma^0 \pi^+$, where λ_i indicates the helicity values for the corresponding hadron.

level	decay	helicity angle	helicity amplitude
0	$e^+e^- \rightarrow \Lambda_c^+(\lambda_1)\Lambda_c^-(\lambda_2)$	θ_0	A_{λ_1,λ_2}
1	$\Lambda_c^+ \rightarrow \Sigma^0(\lambda_3)\pi^+$	(θ_1, ϕ_1)	B_{λ_3}
2	$\Sigma^0 \rightarrow \Lambda(\lambda_4)\gamma(\lambda_5)$	(θ_2, ϕ_2)	C_{λ_4,λ_5}
3	$\Lambda \rightarrow p(\lambda_6)\pi^+$	(θ_3, ϕ_3)	F_{λ_4}

197 $p\pi^-$ planes, while θ_3 is the polar angle of the proton with respect to the opposite direction of the photon momentum
 198 (from $\Sigma^0 \rightarrow \Lambda\gamma$) in the rest frame of Λ .

199 The helicity angles and amplitudes are defined in Table IV. The joint angular dependence of the decay rate is
 200 expressed as

$$\begin{aligned}
 & \frac{d\Gamma}{d\cos\theta_0 d\cos\theta_1 d\cos\theta_2 d\cos\theta_3 d\phi_1 d\phi_2} \\
 & \propto 2 + 2\alpha_0 \cos^2\theta_0 \\
 & - \sqrt{1 - \alpha_0^2} \alpha_\Lambda \sin(2\theta_0) \sin\theta_1 \cos\theta_2 \cos\theta_3 \sin\phi_1 \sin\Delta_0 \\
 & - \sqrt{1 - \alpha_0^2} \alpha_\Lambda \sin(2\theta_0) \cos\theta_1 \sin\theta_2 \cos\theta_3 \sin\Delta_0 \sqrt{1 - (\alpha_{\Sigma^0\pi^+}^+)^2} \sin(\Delta_1^{\Sigma^0\pi^+} + \phi_2) \\
 & - \sqrt{1 - \alpha_0^2} \alpha_\Lambda \sin(2\theta_0) \cos\phi_1 \sin\theta_2 \cos\theta_3 \sin\Delta_0 \sqrt{1 - (\alpha_{\Sigma^0\pi^+}^+)^2} \sin(\Delta_1^{\Sigma^0\pi^+} - \phi_2) \\
 & + \sqrt{1 - \alpha_0^2} \sin(2\theta_0) \sin\theta_1 \sin\phi_1 \sin\Delta_0 \alpha_{\Sigma^0\pi^+}^+ \\
 & - 2\alpha_0 \alpha_\Lambda \cos^2\theta_0 \cos\theta_2 \cos\theta_3 \alpha_{\Sigma^0\pi^+}^+ - 2\alpha_\Lambda \cos\theta_2 \cos\theta_3 \alpha_{\Sigma^0\pi^+}^+.
 \end{aligned} \tag{13}$$

201 where $\Delta_1^{\Sigma^0\pi^+}$ is the phase angle difference for the helicity amplitudes $B_{\frac{1}{2}}$ and $B_{-\frac{1}{2}}$. For the corresponding charge-
 202 conjugate $\bar{\Lambda}_c^-$ decays, one has a similar formula, but with replacements $\bar{\alpha}_\Lambda = -\alpha_\Lambda$, $\bar{\alpha}_{\Sigma^0\pi^-}^- = -\alpha_{\Sigma^0\pi^+}^+$, $\bar{\Delta}_0 =$
 203 Δ_0 , $\bar{\Delta}_1^{\Sigma^0\pi^-} = -\Delta_1^{\Sigma^0\pi^+}$

204 If the phase spaces of level-2 and level-3 decays $\Omega_2=(\theta_2, \phi_2)$ and $\Omega_3=(\theta_3, \phi_3)$ are integrated out, one get the angular
 205 distribution

$$\frac{d\Gamma}{d\cos\theta_0 d\cos\theta_1 d\phi_1} \propto 1 + \alpha_0 \cos^2\theta_0 + \mathcal{P}_T \alpha_{\Sigma^0\pi^+}^+ \sin\theta_1 \sin\phi_1, \tag{14}$$

$$\mathcal{P}_T = \sqrt{1 - \alpha_0^2} \cos\theta_0 \sin\theta_0 \sin\Delta_0. \tag{15}$$

206 Equation (11) becomes in the same forms of Eqs. (4) and (7). If the θ_2 and θ_3 angles are only measured, one has

$$\frac{dN}{d\cos\theta_2 d\cos\theta_3} \propto 1 - \alpha_{\Sigma^0\pi^+}^+ \alpha_\Lambda \cos\theta_2 \cos\theta_3. \tag{16}$$

207 This formula provides a way to measure the decay asymmetry parameter $\alpha_{\Sigma^0\pi^+}^+$ with no information of \mathcal{P}_T .

208 [1] T. D. Lee and C. N. Yang, Phys. Rev., **108**, 1645 (1957).

209 [2] Group Theory, Academic Press, New York, 1959.